

# Fluid Dynamics of the Environment

Lecturers: Stuart Dalziel, Andy Woods and Nathalie Vriend  
Notes by Jonathan Michael Foonlan Tsang

October 19, 2015

These notes are primarily based on the course as it was given in Michaelmas 2014 by Stuart Dalziel and Nathalie Vriend, or on the Michaelmas 2015 version by Dalziel, Vriend and Woods. The headings in the table of contents reflect the official structure of the course, except in §6. An asterisk denotes a section which was either not lectured or not examinable in 2014, but this will not necessarily be true for other years.

The contents of these notes are *not* official.

In the past, this course was known as ‘Geophysical and Environmental Fluid Dynamics’, ‘Environmental Fluid Dynamics’, or a variety of other names.

# Contents

<b>1</b>	<b>Internal gravity waves</b>	<b>7</b>
1.1	The minimal mathematics version . . . . .	7
1.2	A more rigorous derivation . . . . .	8
1.3	Wave velocities . . . . .	9
1.4	Motion of fluid particles . . . . .	10
1.5	Equipartition of energy . . . . .	10
1.6	Oscillating cylinders . . . . .	11
1.7	Reflections . . . . .	11
1.7.1	Properties of reflected beams . . . . .	11
1.7.2	Energy density upon reflection . . . . .	13
1.7.3	Subcritical and supercritical reflections . . . . .	13
1.8	Ray tracing . . . . .	13
1.9	Wave attractors . . . . .	13
1.9.1	Rectangular basins . . . . .	13
1.9.2	Trapezoidal basin . . . . .	13
1.9.3	More complex geometries . . . . .	13
1.9.4	Energy spectrum for attractor . . . . .	13
1.10	Decay along a beam . . . . .	13
1.11	Reflections from rough topology . . . . .	15
1.11.1	Subcritical reflection from a sinusoidal . . . . .	15
1.11.2	Supercritical reflections from a sinusoidal . . . . .	15
1.12	Non-linear stratification . . . . .	15
1.12.1	Very sharp changes . . . . .	15
1.12.2	Very slow changes . . . . .	16
1.13	Leewaves . . . . .	16
1.13.1	Kelvin ship waves . . . . .	16
1.13.2	Extended range of hills . . . . .	17
1.13.3	Causality . . . . .	17
1.14	Shear flows . . . . .	17
1.14.1	Sheared base state . . . . .	17
1.14.2	Ray tracing in a shear flow . . . . .	18
1.14.3	*Three-dimensional forcing . . . . .	18
1.14.4	*Effect of viscosity . . . . .	18
1.14.5	*Blocking . . . . .	18
1.15	Columnar modes . . . . .	18
1.16	*Stokes drift in internal waves . . . . .	18
1.17	Resonant triads . . . . .	18
<b>2</b>	<b>Turbulence primer</b>	<b>19</b>
2.1	Basics of turbulence . . . . .	19
2.1.1	What is turbulence? . . . . .	19
2.1.2	Vortex stretching . . . . .	19
2.1.3	Energy dissipation: Kolmogorov's theory (1941) . . . . .	20
2.1.4	Two-dimensional turbulence . . . . .	21
2.2	Simplistic approaches to modelling turbulence . . . . .	21

2.2.1	Molecular diffusion . . . . .	22
2.2.2	The closure problem . . . . .	22
2.2.3	The $k$ - $\epsilon$ model . . . . .	23
2.2.4	Turbulent diffusion models . . . . .	23
2.2.5	Prandtl's mixing length model . . . . .	24
2.2.6	Entrainment: Diffusion of turbulence . . . . .	24
2.3	Mixing . . . . .	24
2.3.1	What is mixing? . . . . .	24
2.3.2	The energy budget . . . . .	25
2.4	*Stably stratified flows . . . . .	26
2.4.1	Stratification modifies turbulence . . . . .	26
2.5	*Mixing efficiency . . . . .	26
2.6	*Internal mixing . . . . .	26
2.6.1	Kelvin-Helmholtz instability . . . . .	26
2.6.2	Stratified shear flow . . . . .	26
2.6.3	Holmboe instability . . . . .	26
2.6.4	Entrainment by internal mixing . . . . .	26
<b>3</b>	<b>Shallow water</b> . . . . .	<b>27</b>
3.1	Introduction . . . . .	28
3.2	Linear waves on an interface . . . . .	28
3.2.1	Dispersion relation . . . . .	28
3.2.2	Properties of interfacial waves . . . . .	28
3.2.3	The short wave limit . . . . .	28
3.2.4	The long wave limit . . . . .	28
3.2.5	Energy . . . . .	28
3.3	Shallow water equations . . . . .	28
3.3.1	Mathematical definition of 'shallow' . . . . .	28
3.3.2	Derivation from first principles . . . . .	28
3.3.3	Boussinesq versus non-Boussinesq . . . . .	28
3.3.4	More than one layer . . . . .	28
3.3.5	Derivation by averaging . . . . .	28
3.4	Hyperbolic systems . . . . .	28
3.4.1	A model for traffic flow . . . . .	28
3.4.2	Shallow water as a hyperbolic system . . . . .	28
3.4.3	Matrix formulation . . . . .	28
3.4.4	General approach to hyperbolic systems . . . . .	28
3.4.5	Implications of hyperbolic nature . . . . .	28
3.4.6	The dam break problem . . . . .	29
3.4.7	Entrainment into shallow water flows . . . . .	30
3.5	Gravity currents . . . . .	33
3.5.1	A moving dam problem . . . . .	33
3.5.2	Description . . . . .	33
3.5.3	Early models . . . . .	33
3.5.4	Cavity flows . . . . .	33
3.5.5	*Morden and Beiburg . . . . .	33
3.5.6	Gravity currents and characteristics . . . . .	33
3.5.7	Modelling gravity currents . . . . .	33
3.5.8	Real life is more complex . . . . .	33
<b>4</b>	<b>Jets, plumes and thermals</b> . . . . .	<b>35</b>
4.1	Jets . . . . .	35
4.2	General plume equations . . . . .	36
4.2.1	Self-similar plumes . . . . .	36
4.2.2	Time-dependent plume equations . . . . .	37
4.3	Plumes in a homogeneous environment . . . . .	37
4.3.1	Steady Boussinesq plumes . . . . .	37

4.3.2	Time-dependent plumes . . . . .	37
4.3.3	Steady non-Boussinesq plumes . . . . .	37
4.4	Plumes in a stratified environment . . . . .	37
4.4.1	Rise height . . . . .	38
4.4.2	Series solution in Boussinesq fluid . . . . .	38
4.5	*Thermal in a homogeneous environment . . . . .	38
4.6	*Thermals in a stratified environment . . . . .	38
<b>5</b>	<b>Buoyancy-driven flows</b>	<b>39</b>
<b>6</b>	<b>Particle-laden and granular flow</b>	<b>41</b>
6.1	Types of particulate flows . . . . .	41
6.2	Physics within a particle gravity current . . . . .	42
6.3	Sedimenting particle-laden flows . . . . .	42
6.3.1	Type I: Free settling of individual particles . . . . .	43
6.3.2	Type II: Flocculent settling, particle coalescence . . . . .	45
6.3.3	Type III: Hindered (zone) settling . . . . .	45
6.3.4	Type IV: Compressional settling, compacting . . . . .	45
6.4	Modelling a particulate gravity current . . . . .	46
6.4.1	A simple box model . . . . .	46
6.5	Sediment transport . . . . .	47
6.5.1	Resuspension . . . . .	47
6.6	Aqueous and aeolian bedforms (dunes) . . . . .	47
6.7	Dry granular flows, rheology, segregation . . . . .	47



# Chapter 1

## Internal gravity waves

In a *stratified fluid* with variable density (such as an ocean, in which we have dense salty water at the bottom and lighter, fresh water at the top), it is possible to sustain *internal gravity waves* in addition to surface waves.

### 1.1 The minimal mathematics version

Consider a parcel of fluid in a stable stratification. If the parcel is raised from its original position, then it will be heavier than the surrounding fluid, and will sink back down. If it is lowered, then buoyancy will push it back up. Thus density differences provide a restoring force to a parcel displaced vertically.

Let  $\rho(z)$  be the density of the fluid, with  $z$  vertically upwards. We then have  $\frac{d\rho}{dz} < 0$  since the stratification is stable. If the parcel has volume  $V$  and is displaced upwards by  $H$ , then the density difference between the parcel and the surrounding fluid is

$$\Delta\rho = \frac{d\rho}{dz} H \quad (1.1.1)$$

and the downwards force on the parcel is therefore

$$F = gV\Delta\rho = gV \frac{d\rho}{dz} H \quad (1.1.2)$$

Meanwhile, the mass of the particle is

$$m = \rho V \quad (1.1.3)$$

and so Newton's law  $F = ma$  gives the acceleration

$$a = \frac{g}{\rho} \frac{d\rho}{dz} H \quad (1.1.4)$$

which is in the opposite direction to the displacement.

We assume that the fluid is *Boussinesq*<sup>1</sup>, so that fluid accelerations are small compared to gravity. We also assume that any density differences are small compared to a reference density  $\rho_0$ . Thus, we will make the approximation  $\rho \approx \rho_0$  except when densities are multiplied by gravity. We define the *buoyancy frequency* (or *Brunt-Väisälä frequency*)  $N$  by

$$N = \sqrt{-\frac{g}{\rho_0} \frac{d\rho}{dz}}. \quad (1.1.5)$$

Then

$$a = -N^2 H \quad (1.1.6)$$

so parcels of fluid execute oscillations with frequency  $\omega = N$ .

---

<sup>1</sup>After Joseph Valentin Boussinesq (1842–1929)

The above argument is not quite valid, because we have neglected *continuity*. We cannot simply displace a parcel of fluid without displacing some other fluid around it. Instead, we could consider displacing an entire vertical slab of fluid and making it oscillate in its plane. Following the same steps gives the same result.

In the oceans,  $N \approx 10^{-2}\text{s}^{-1}$ .

Suppose we now take a slab of fluid which makes an angle  $\theta$  with the vertical, and we displace it by a distance  $d$  along its plane. To maintain continuity, the slab must oscillate in its plane (rather than falling straight down).

The vertical displacement of the slab is  $d \cos \theta$ . The restoring force in the direction of the displacement is therefore proportional to  $\cos^2 \theta$ . A similar argument to the above shows that the slab will execute oscillations with frequency

$$\omega = N \cos \theta. \quad (1.1.7)$$

This is the dispersion relation for internal gravity waves, and we will see this many times. Note that the frequency  $\omega$  depends on the orientation of the wave, but not at all on the wavenumber or wavelength.

## 1.2 A more rigorous derivation

We can derive the above more rigorously by starting from the governing equations of an incompressible<sup>2</sup> inviscid<sup>3</sup> fluid:

$$\nabla \cdot \mathbf{u} = 0 \quad (1.2.1)$$

$$\rho_t + \nabla \cdot (\rho \mathbf{u}) = 0 \quad (1.2.2)$$

$$(\rho \mathbf{u})_t + \nabla \cdot (\rho \mathbf{u} \mathbf{u}) = -\nabla p + \rho \mathbf{g} \quad (1.2.3)$$

These are the equations for conservation of volume, mass and momentum respectively. The conservative forms may also be expanded as

$$\nabla \cdot \mathbf{u} = 0 \quad (1.2.4)$$

$$\rho_t + \mathbf{u} \cdot \nabla \rho = 0 \quad (1.2.5)$$

$$\rho(\mathbf{u}_t + \mathbf{u} \cdot \nabla \mathbf{u}) = -\nabla p + \rho \mathbf{g}. \quad (1.2.6)$$

We linearise the governing equations for small displacements, velocities and density perturbations from the stationary stratified state, writing

$$\rho = \bar{\rho}(z) + \rho' \quad (1.2.7)$$

$$p = \bar{p}(z) + p' \quad (1.2.8)$$

and assume that the primed quantities and  $\mathbf{u}$  are ‘small’.<sup>4</sup> Then linearising the governing equations gives

$$\nabla \cdot \mathbf{u} = 0 \quad (1.2.9)$$

$$\frac{d\bar{p}}{dz} = -g\bar{\rho} \quad (1.2.10)$$

$$\rho'_t = -w \frac{d\bar{\rho}}{dz} \quad (1.2.11)$$

$$\bar{\rho} \mathbf{u}_t = -\nabla p' - g\rho' \mathbf{e}_z. \quad (1.2.12)$$

Note that (1.2.10) simply says that in the unperturbed state, the pressure is hydrostatic.

For a Boussinesq fluid,  $\rho \approx \rho_0$  except when multiplied by  $g$ , so the momentum equation (1.2.12) becomes

$$\mathbf{u}_t = -\frac{1}{\rho_0} \nabla p' - \frac{g}{\rho_0} \rho' \mathbf{e}_z. \quad (1.2.13)$$

---

<sup>2</sup>i.e. low Mach number

<sup>3</sup>i.e. high Reynolds number

<sup>4</sup>Is this safe?



Take  $\nabla \cdot (1.2.13)$  and use  $\nabla \cdot \mathbf{u} = 0$  to get

$$\nabla^2 p' = -g \frac{\partial \rho'}{\partial z} \quad (1.2.14)$$

and then take  $\nabla^2$  of the  $z$ -component of (1.2.13) to get

$$\nabla^2 w_t = -\frac{g}{\rho_0} (\rho'_{zz} - \nabla^2 \rho') \quad (1.2.15)$$

Differentiating with respect to time and using the equation for  $\rho'_t$  gives

$$\nabla^2 w_{tt} = \frac{g}{\rho_0} \left( \nabla^2 - \frac{\partial^2}{\partial z^2} \right) (w \bar{\rho}_z) \quad (1.2.16)$$

$$\approx N^2 \left( \frac{\partial^2}{\partial z^2} - \nabla^2 \right) w \quad (1.2.17)$$

where the approximation applies for a Boussinesq fluid.

**Plane wave eigenvalue problem** We can solve this linear PDE with constant coefficients by considering the normal modes. If we write

$$w = \hat{w} \exp(i(\mathbf{k} \cdot \mathbf{x} - \omega t)) \quad (1.2.18)$$

where  $\mathbf{k} = (k, l, m)$ , then we get the dispersion relation

$$\omega^2 = N^2 \frac{k^2 + l^2}{k^2 + l^2 + m^2} \quad (1.2.19)$$

How do we relate this to the argument with slabs, and recover (1.1.7)? We note that the slabs were lines of constant phase, i.e. of constant  $\mathbf{k} \cdot \mathbf{x}$ . So  $\mathbf{k}$  is perpendicular to the slab. Hence if the slab makes an angle  $\theta$  with the upwards vertical, then  $\mathbf{k}$  makes an angle  $\theta$  with the horizontal, and so

$$\cos \theta = \frac{k^2 + l^2}{k^2 + l^2 + m^2} \quad (1.2.20)$$

as required.

**Evanescent waves** Note that if  $\omega > N$  then there are no real solutions to (1.2.19). Rather,  $(k, l, m)$  must be complex and have an imaginary component, which means  $e^{i\mathbf{k} \cdot \mathbf{x}}$  decays exponentially as  $\mathbf{x}$  increases in a certain direction. Such ‘waves’ are called *evanescent waves*. A source which oscillates at a frequency  $\omega$  will cause localised disturbances. Energy is not carried away.

### 1.3 Wave velocities

From the dispersion relation, we obtain the phase and group velocities in the usual way:

$$\mathbf{c}_p = \frac{\omega}{|\mathbf{k}|} \hat{\mathbf{k}} \quad (1.3.1)$$

$$= \frac{N}{k} \cos \theta \hat{\mathbf{k}} \quad (1.3.2)$$

$$= N \sqrt{\frac{k^2 + l^2}{k^2 + l^2 + m^2}} (k, l, m) \quad (1.3.3)$$

and

$$\mathbf{c}_g = \frac{\partial \omega}{\partial \mathbf{k}} \quad (1.3.4)$$

$$= -N \sin \theta \frac{\partial \theta}{\partial \mathbf{k}} \quad (1.3.5)$$

$$= \frac{N}{|\mathbf{k}|^3 \sqrt{k^2 + l^2}} (km^2, lm^2, -(k^2 + l^2)m) \quad (1.3.6)$$

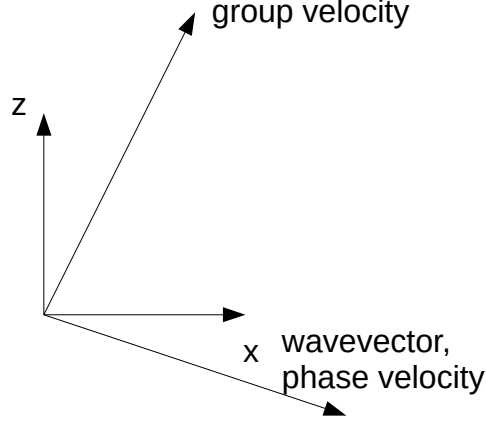


Figure 1.1: The geometric relationship between phase velocity, group velocity and wavevector.

Note that

$$\mathbf{c}_p \cdot \mathbf{c}_g = 0 \quad (1.3.7)$$

so the phase and group velocities are perpendicular. Moreover, the group and phase velocities have  $z$ -components in opposite directions. See figure 1.1.

The phase velocity is the velocity at which crests move, or more abstractly the velocity at which ‘phase is advected’. The group velocity is the velocity with which wavepackets propagate, and can be interpreted as a rate and direction of energy transfer. The group velocity makes an angle  $\theta$  with the vertical.

## 1.4 Motion of fluid particles

For simplicity, we consider two-dimensional motion. If  $\mathbf{u} = (u, 0, w)$  and

$$u = \hat{u} \exp(i(\mathbf{k} \cdot \mathbf{x} - \omega t)) \quad (1.4.1)$$

$$w = \hat{w} \exp(i(\mathbf{k} \cdot \mathbf{x} - \omega t)) \quad (1.4.2)$$

$$(1.4.3)$$

then  $\nabla \cdot \mathbf{u} = 0$  gives

$$\hat{u} = -\frac{m}{k} \hat{w} \quad (1.4.4)$$

which tells us that fluid particles oscillate parallel to the group velocity and perpendicularly to the wavevector. We can obtain the displacements by integrating with respect to time, or equivalently by dividing by  $-i\omega$ .

## 1.5 Equipartition of energy

Dotting (1.2.13) with  $\mathbf{u}$  and some manipulation gives us

$$\frac{\partial}{\partial t} \left( \frac{1}{2} \rho_0 \mathbf{u}^2 + \frac{1}{2} \frac{g^2}{\rho_0 N^2} \rho'^2 \right) + \nabla \cdot (p' \mathbf{u}) = 0, \quad (1.5.1)$$

the equation of conservation of energy. We identify  $\frac{1}{2}\rho_0\mathbf{u}^2$  as kinetic energy density and  $\frac{1}{2}\frac{g^2}{\rho_0 N^2}\rho'^2$  as potential energy density. (Energy density is energy per unit volume, with dimensions  $\text{L}^{-1}\text{T}^{-2}$ .) And we identify  $p'\mathbf{u}$  as the flux of energy per unit area.

In integral form, we can write

$$\frac{\partial}{\partial t} \int_V (KE + PE) dV + \int_S \mathbf{F}_E \cdot \mathbf{n} dS = 0 \quad (1.5.2)$$

where  $KE$  is the kinetic energy density,  $PE$  is the potential energy density, and  $\mathbf{F}_E$  is the energy flux.

Consider a normal mode with phase  $\phi' = \mathbf{k}' \cdot \mathbf{x}' - \omega t$ . In a rotated coordinate system, where  $w'$  now means the velocity component along the wave ray, we have

$$w' = \omega \eta_0 \sin \phi' \quad (1.5.3)$$

$$b = \frac{-\omega^2 \eta_0}{\cos \theta} \cos \phi' \quad (1.5.4)$$

$$p' = \frac{-\rho_0 \omega^2 \eta_0 \tan \theta}{k'} \sin \phi' \quad (1.5.5)$$

with the other two components of velocity being zero. Thus

$$KE = \frac{1}{2} \rho_0 \omega^2 \eta_0^2 \sin^2 \phi' \quad (1.5.6)$$

$$PE = \frac{1}{2} \rho_0 \omega^2 \eta_0^2 \cos^2 \phi'. \quad (1.5.7)$$

Calculating time averages shows that

$$\langle \text{kinetic energy density} \rangle = \langle \text{potential energy density} \rangle \quad (1.5.8)$$

which is *equipartition of energy*.

The energy flux is  $\mathbf{F}_E = \rho_0 \omega^2 \eta_0^2 \sin^2 \phi' \mathbf{c}_g$ , and so  $\bar{\mathbf{F}}_E = \bar{E} \mathbf{c}_g$ . Thus the energy flux is in the direction of the group velocity. Note that we must take real parts before multiplying together any quantities.

## 1.6 Oscillating cylinders

Consider a cylinder (or any other object) suspended in a stratified medium.

At time  $t = 0$ , it is impulsively started to oscillate at frequency  $\omega < N$ . The impulsive start of the cylinder generates an entire spectrum of transient wave modes, which generates IGWs propagating at different values of  $\theta$ .<sup>5</sup> After some time, when the transients have decayed or moved away, we will see a single mode of IGWs propagating at  $\theta = \cos^{-1}(\omega/N)$  to the vertical.

If the cylinder is made to oscillate at a frequency  $\omega > N$ , then the waves produced will be evanescent. The cylinder will create local disturbances which do not travel very far.

## 1.7 Reflections

### 1.7.1 Properties of reflected beams

At a boundary, the normal velocity component must be continuous. For a rigid stationary boundary, this means that the normal velocity component must vanish.

---

<sup>5</sup>Consider the Fourier transform of the Heaviside step function.

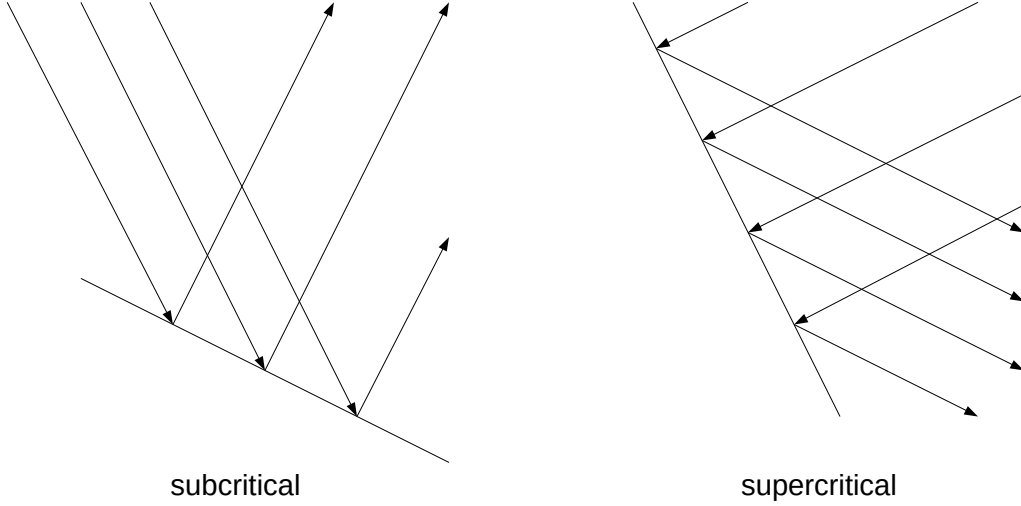


Figure 1.2: Super- and sub-critical reflections.

Suppose  $z = 0$  is a rigid stationary boundary, with a plane wave incident from  $z > 0$ . What is the reflected wave? We have

$$w = w_I + w_R \quad (1.7.1)$$

$$w_I = \hat{w}_I \exp(i(\mathbf{k}_I \cdot \mathbf{x} - \omega t)) \quad (1.7.2)$$

$$w_R = \hat{w}_I \exp(i(\mathbf{k}_R \cdot \mathbf{x} - \omega t)); \quad (1.7.3)$$

the two waves must have the same  $\omega$  and  $k_I = k_R$ ; the boundary condition gives  $\hat{w}_I + \hat{w}_R = 0$ . And causality implies that  $m_R = -m_I$ .

When a plane wave reflects off a flat boundary, the incident and reflected waves make the same angle (but reflected) with the vertical or horizontal, so that the two waves have the same frequency  $\omega = N \cos \theta$ . (Note that for IGWs,  $\theta$  always represents the angle between a wave's direction and the vertical.) In general, the angle of incidence and angle of reflection are not equal. Depending on how the angle of the incident wave compares with the slope of the boundary, one of two things may happen: see Figure 1.2.

From Figure 1.2 we can see that reflections change the wavenumber of the wave and can act to focus or defocus the rays, depending on direction. Let  $\alpha$  be the angle that the plane boundary makes with the vertical. We define the quantity

$$\gamma = \frac{\sin(\alpha - \theta)}{\sin(\alpha + \theta)} \quad (1.7.4)$$

to characterise the *focusing power* of a reflection.

After a lot of manipulation, we can show that focusing reflections change the amplitude and wavenumber according to

$$k_R = \gamma k_I \quad (1.7.5)$$

$$A_R = \gamma A_I \quad (1.7.6)$$

and that defocusing reflections have the opposite effect:

$$k_R = \gamma^{-1} k_I \quad (1.7.7)$$

$$A_R = \gamma^{-1} A_I. \quad (1.7.8)$$

Thus the magnitudes of the phase velocity and group velocity change as well, since

$$|\mathbf{c}_p| = \frac{N}{|\mathbf{k}|} \cos \theta \quad (1.7.9)$$

$$|\mathbf{c}_g| = \frac{N}{|\mathbf{k}|} \sin \theta \quad (1.7.10)$$

### 1.7.2 Energy density upon reflection

The energy density per unit wavelength is

$$\tilde{E} \sim \lambda A^2. \quad (1.7.11)$$

After a focusing reflection,  $\lambda$  is divided by  $\gamma$  but  $A$  is multiplied by  $\gamma$ , so  $\tilde{E}$  is multiplied by  $\gamma$ . Hence the energy density per wavelength is increased after a focusing reflection.

The energy density per unit length is

$$\hat{E} = \frac{1}{\lambda} \tilde{E} \quad (1.7.12)$$

and so  $\hat{E}$  is multiplied by  $\gamma^2$  after a focusing reflection.

### 1.7.3 Subcritical and supercritical reflections

In a subcritical reflection, the boundary has a shallower slope than the wave ( $\theta < \alpha$ ), and the vertical propagation of the wave is reversed by the reflection. The horizontal direction of propagation is maintained.

In a supercritical reflection,  $\theta > \alpha$  and the vertical direction of propagation is maintained but the horizontal direction is reversed.

When  $\theta$  and  $\alpha$  are very similar, then  $\gamma$  becomes very large. Waves will have very large amplitudes, and nonlinear effects and viscosity, which we had ignored from the outset, become important.

## 1.8 Ray tracing

Since the frequency  $\omega$  is preserved upon reflection, the angle to the vertical  $\theta$  is conserved. Waves therefore tend to propagate along well-defined rays. The dispersion relation alone does not tell us which way a wave propagates. We must pay attention to *causality*, the fact that waves propagate away from whatever generates a disturbance.

Our analysis so far deals with waves which are a linear perturbation from an equilibrium configuration. We have seen that when a wave reflects from a rigid surface, the reflected wave may have a larger amplitude than the incident wave. Depending on the shape of the domain and its boundaries, repeated reflections may increase the amplitude of waves and cause nonlinear effects to become important. In particular, repeated reflections can lead to trapping, to amplitudes increasing, and eventually to wave-breaking.

## 1.9 Wave attractors

### 1.9.1 Rectangular basins

### 1.9.2 Trapezoidal basin

### 1.9.3 More complex geometries

### 1.9.4 Energy spectrum for attractor

## 1.10 Decay along a beam

So far we have completely ignored viscosity. But when a beam of waves travels across long distances, a small viscosity may be enough to cause significant energy losses along the beam. In this section, we reintroduce a constant viscosity  $\nu$ , and consider the long-distance behaviour of beams.

The equations of motions are

$$\frac{\partial u}{\partial t} + \frac{1}{\rho_0} \frac{\partial p}{\partial x} = \nu \nabla^2 u \quad (1.10.1)$$

$$\frac{\partial w}{\partial t} + \frac{1}{\rho_0} \frac{\partial p}{\partial z} - b = \nu \nabla^2 w \quad (1.10.2)$$

$$\frac{\partial b}{\partial t} + N^2 w = 0 \quad (1.10.3)$$

$$\nabla \cdot \mathbf{u} = 0 \quad (1.10.4)$$

where

$$b = \frac{-g}{\rho_0} (\rho - \rho_0) \quad (1.10.5)$$

is the buoyancy.

Introduce a streamfunction  $\psi$  such that  $(u, w) = (-\psi_z, \psi_x)$ . We have

$$\frac{\partial b}{\partial t} + N^2 \frac{\partial \psi}{\partial x} = 0 \quad (1.10.6)$$

$$\frac{\partial}{\partial t} \nabla^2 \psi - \frac{\partial b}{\partial t} - \nu \nabla^4 \psi = 0 \quad (1.10.7)$$

Then some cross-differentiation eliminates  $p$  and  $b$  to give

$$\nabla^2 \psi_{tt} + N^2 \psi_{xx} = \nu \nabla^4 \psi_t. \quad (1.10.8)$$

The  $\nu \nabla^4 \psi_t$  term acts to damp waves. We could look for plane-wave solutions to (1.10.8) in the usual way, and obtain the dispersion relation

$$\omega^2 + i\nu(k^2 + m^2) - N^2 \cos^2 \theta = 0 \quad (1.10.9)$$

where  $\cos \theta = k/|\mathbf{k}|$  as usual. Given  $(k, m)$ , we could solve (1.10.9) for  $\omega$ .

But often we are more interested in the spatial decay of a beam that is generated by oscillations at a fixed  $\omega$ . We expect that the beam would still propagate in the direction  $\theta = \cos^{-1}(\omega/N)$ , but with a decaying amplitude. Thus we define a scaled coordinate  $\chi = \frac{\epsilon}{\sin \theta} \xi$ , where  $\xi$  is the unscaled coordinate along the beam.

We let  $\epsilon = \nu/2$  and we expand  $\psi$  and  $b$  as perturbation series:

$$\psi = (\psi_0 + \epsilon \psi_1 + \dots) \exp(i\omega t) \quad (1.10.10)$$

$$b = (b_0 + \epsilon b_1 + \dots) \exp(i\omega t). \quad (1.10.11)$$

Substituting into the governing equations and comparing orders of  $\epsilon$  gives us

$$\frac{\partial^4 \psi_0}{\partial \zeta^4} = i \frac{\partial^2 \psi_0}{\partial \zeta \partial \chi} \quad (1.10.12)$$

and some work will give

$$\psi_0 = A \exp(ik\zeta - k^3 \chi) \quad (1.10.13)$$

for some constant  $A$ . Thus the velocity decays exponentially along the beam; waves with higher wavenumbers decay faster. In the environment, IGWs have wavelengths on the order of hundreds of metres, but in the lab the wavelengths are much smaller, on the order of a few centimetres.

We could also consider energy losses due to the diffusion of buoyancy (or equivalently of temperature) instead of the diffusion of momentum. In practice, both effects may be important. The relative importance of the two diffusion processes is quantified by the Prandtl number  $\text{Pr} = \nu/\kappa$ .

## 1.11 Reflections from rough topography

Consider a wave beam of wavenumber  $k_0$ , making an angle  $\theta$  with the vertical, reflecting from a sinusoidal topography

$$z = h = h_0 \sin k_T x \quad (1.11.1)$$

where  $k_T$  is the ‘wavenumber’ of the topography. The incident beam is propagating downwards and to the right. We suppose that the height of the topography,  $h_0$ , is small (more precisely, that  $h_0 k_T \ll 1$ ).

Suppose the incident beam would reach  $z = 0$  at  $x = x_0$ , were it not for the topography. The equation of the beam is therefore given by

$$z = \beta(x_0 - x) \quad (1.11.2)$$

where  $\beta = 1/\tan \theta$ . The beam intersects the topography at the point  $x = x_i$ , where  $x_i$  solves

$$h_0 \sin k_T x_i = \beta(x_0 - x_i). \quad (1.11.3)$$

Define  $\delta x = x_i - x_0$

### 1.11.1 Subcritical reflection from a sinusoidal

If the slope of the topography is sufficiently small, then all ray reflections will be subcritical and ray tracing suggests that an incident wavebeam should be reflected forwards.

If  $k_0 < k_T$ , so the wavelength of the incident beam is larger than the wavelength of the topography, then we get *back scatter*: The reflected wave propagates upwards but to the *left*. This is because the group velocity of the reflected wave must be upwards.

### 1.11.2 Supercritical reflections from a sinusoidal

**Steep topography** If instead we had steep topography, with  $h_0 k_T \gg 1$ , then the picture is much more complicated. Rays can bounce multiple times off the topography before leaving. We will observe both forward scatter and back scatter. The amounts of energy that scatter forwards and backwards depends very sensitively on the incident angle  $\theta$ , and it is not possible to write down a formula for these amounts (although it is possible to bound them).

Moreover, attractors may form in the deep gaps between the topography. These may cause the amplitude of the wave to increase so much that wave breaking starts to occur. The inviscid approximation also becomes invalid, because steep velocity gradients will form. Mixing may occur, destroying the original stratification.

## 1.12 Non-linear stratification

If  $N$  is not constant but varies with  $z$  (say), then waves will not follow straight paths but will refract, and may also reflect.

### 1.12.1 Very sharp changes

Consider a stratification with  $N = N_1$  in  $z < 0$  and  $N = N_2$  in  $z > 0$ , where  $N_2 < N_1$ . Consider a wave incident from  $z < 0$  with frequency  $\omega$ . The incident wave’s angle to the vertical  $\theta_i$  is given by  $\cos \theta_i = \omega/N_1$ . A transmitted wave in  $z > 0$  will make an angle  $\theta_t$  to the vertical, where  $\cos \theta_t = \omega/N_2$ . In order that the boundary conditions be satisfied, there will also need to be a *reflected* wave propagating downwards from  $z = 0$ . Thus we have *total internal reflection*.

Note that if  $N_2 < \omega < N_1$  then the transmitted wave will be evanescent.

### 1.12.2 Very slow changes

If  $N$  varies very slowly with  $z$ , over lengthscales much larger than a wavelength, then the WKB method can be used to find the trajectory of a wave.

The frequency  $\omega$  of a wave is still constant, and we assume that  $\omega$  is still related to  $\theta$ , the angle between the direction of propagation and the vertical, by

$$\omega = N(z) \cos \theta. \quad (1.12.1)$$

Since  $\omega$  is fixed, this determines  $\theta = \theta(z)$ , which allows us to solve for the path of the ray. Say the ray is given by  $x = X(z)$ . Then

$$\frac{dX}{dz} = \tan \theta = \frac{\sqrt{1 - \cos^2 \theta}}{\cos \theta}. \quad (1.12.2)$$

For example, consider  $N(z) = N_0 e^{-z/H}$ , so that  $\cos \theta(z) = (\omega/N_0) e^{z/H}$ . Then we have

$$\frac{dX}{dz} = \sqrt{1 - \cos^2 \theta_0} e^{2z/H} \frac{e^{-z/H}}{\cos \theta_0}. \quad (1.12.3)$$

As  $z$  increases,  $N$  decreases. Eventually we will have  $\omega/N \rightarrow 1$ ,  $\frac{dX}{dz} \rightarrow \infty$  and the wave can no longer propagate upwards. Instead, the wave is reflected back downwards. (In practice, the amplitude of the wave also grows as we approach  $\omega/N \rightarrow 1$ , so that nonlinear processes start to play a role as well.)

## 1.13 Leewaves

When a medium flows past an obstacle and waves are formed in the wake, it is possible to get standing waves (also known as stationary waves). When standing IGWs occur in the atmosphere as a wind flows past obstacles such as mountains, these are known as leewaves.

### 1.13.1 Kelvin ship waves

As an aside to introduce standing waves, we consider a ship moving with velocity  $\mathbf{U} = U \mathbf{e}_x$  in deep water. The surface waves in deep water have a dispersion relation

$$\omega^2 = g|\mathbf{k}| \quad (1.13.1)$$

and phase

$$\phi = \mathbf{k} \cdot \mathbf{x} - \omega t. \quad (1.13.2)$$

Let  $\mathbf{x}'$  denote a position vector relative to the ship, so that  $\mathbf{x}' = \mathbf{x} - \mathbf{U}t$ . Then

$$\phi = \mathbf{k} \cdot \mathbf{x}' + (\mathbf{k} \cdot \mathbf{U} - \omega)t. \quad (1.13.3)$$

Hence waves that are stationary in the frame of the ship have

$$\mathbf{k} \cdot \mathbf{U} = \omega \quad (1.13.4)$$

$$U \cos \theta = |\mathbf{c}_g| \quad (1.13.5)$$

where, in this section,  $\theta$  is the angle between  $\mathbf{U}$  and  $\mathbf{k}$ .

For these waves,  $\mathbf{c}_g$  and  $\mathbf{c}_p$  are parallel, and  $|\mathbf{c}_g| = \frac{1}{2}|\mathbf{c}_p| = \frac{1}{2}U \cos \theta$ . This is the speed at which wave packets travel. Some geometry then tells us the shape that these waves make behind the ship.

In shallow water, surface waves are not dispersive and such stationary waves are not seen.



### 1.13.2 Extended range of hills

Now we consider leewaves, i.e. stationary atmospheric IGWs as a wind of speed  $U$  flows, from left to right, over a sinusoidal mountain range which has wavelength  $\lambda_T$  and so topographical wavenumber  $k_T = 2\pi/\lambda$ .

An observer in the frame of the mountains sees the leewaves as having a constant phase. The frequency of the forcing must therefore be

$$\omega = k_T U = \frac{2\pi U}{\lambda_T} \quad (1.13.6)$$

and the wave crests make an angle  $\theta = \cos^{-1}(\omega/N)$  with the vertical. The phase velocity is aligned with the wave crests, so that the observer sees the waves as being stationary.

We move to a frame moving with the wind, in which the mountains are moving with speed  $U$  to the left. This does not change the angle between the wave crests and the vertical. But in the new frame the group velocity is  $\mathbf{c}'_g = \mathbf{c}_g - \mathbf{U}$ , and is aligned with the crests.

### 1.13.3 Causality

## 1.14 Shear flows

### 1.14.1 Sheared base state

Suppose the background stratified fluid is not stationary but has velocity  $\mathbf{U} = (U(z), 0, 0)$ . Linearising the full governing equations of motion about this base state by writing  $\mathbf{u} = \mathbf{U} + (u', v', w')$ , and a lot of manipulation to eliminate everything apart from  $w'$ , eventually gives

$$\left(\frac{\partial}{\partial t} + U \frac{\partial}{\partial x}\right)^2 \nabla^2 w' + N^2 \frac{\partial^2 w'}{\partial x^2} - U'' \left(\frac{\partial}{\partial t} + U \frac{\partial}{\partial x}\right) \frac{\partial w'}{\partial x} = 0. \quad (1.14.1)$$

Note that this reduces to 1.2.17 if  $U \equiv 0$ . If  $U$  is constant, then a change of frame would recover 1.2.17 as expected.

For flows which are steady (in this frame of reference), we have

$$\frac{\partial^2}{\partial x^2} \nabla^2 w' + \left(\frac{N^2}{U^2} - \frac{U''}{U}\right) \frac{\partial^2 w'}{\partial x^2} = 0. \quad (1.14.2)$$

Integrating twice with respect to  $x$  then gives

$$\nabla^2 w' + \left(\frac{N^2}{U^2} - \frac{U''}{U}\right) w' = 0. \quad (1.14.3)$$

If  $U$  and  $N$  are constant, or very slowly varying, then we can search for plane wave solutions

$$w' = w_0 e^{i(kx + mz)} \quad (1.14.4)$$

which satisfy

$$-(k^2 + m^2) + \frac{N^2}{U^2} = 0 \quad (1.14.5)$$

or  $|\mathbf{k}| = N/U$  as before. Note that this is also true whenever

$$\frac{N^2}{U^2} - \frac{U''}{U} \quad (1.14.6)$$

is constant.

### 1.14.2 Ray tracing in a shear flow

When the length scale over which  $U$  and  $N$  change is much larger than the wavelength of internal waves, we can consider the important wave properties as being instantaneous in the local state of the background flow. This is the WKB approximation. Rays follow the group velocity relative to the fluid. However, in our frame of reference the waves appear stationary, and so the phase velocity must be parallel to the wave crests and the group velocity antiparallel with the wavenumber vector. We can thus take the trajectory of a wave propagating with the mean flow as

$$\frac{dz}{dx} = \frac{c_{gz}}{U - c_{gx}} = \frac{m}{k} \quad (1.14.7)$$

where  $c_g$  is the group velocity relative to the fluid.

Recalling that  $k^2 + m^2 = N^2/U^2$ , and assuming that  $k$  is conserved along the ray and  $U''/U \ll N^2/U^2$ , then

$$m^2 = \frac{N^2}{U^2} - k^2 \quad (1.14.8)$$

and so

$$\frac{dz}{dx} = \left( \left( \frac{N}{kU} \right)^2 - 1 \right)^{1/2}. \quad (1.14.9)$$

Waves cannot propagate through a level where  $kU/N = 1$ .

In the atmosphere,  $U/N$  tends to increase with height as  $U$  increases.

### 1.14.3 \*Three-dimensional forcing

### 1.14.4 \*Effect of viscosity

### 1.14.5 \*Blocking

## 1.15 Columnar modes

### 1.16 \*Stokes drift in internal waves

### 1.17 Resonant triads

# Chapter 2

## Turbulence primer

Most environmental and geophysical flows occur at high Reynolds numbers. At high Reynolds numbers, steady laminar solutions to the Navier-Stokes equations are extremely unstable, and the flows are turbulent. In transitioning from a steady laminar solution to a fully turbulent solution, a system undergoes a number of bifurcations as the Reynolds number increases beyond critical values. These bifurcations are analogous to Hopf bifurcations, or to the period-doubling bifurcations exhibited by the logistic map.

### 2.1 Basics of turbulence

Throughout this and the next section, we shall assume that the density  $\rho$  is constant and uniform.

#### 2.1.1 What is turbulence?

Although there is no simple definition for turbulence, turbulent flows can be characterised by a few properties:

- Turbulent flows are dominated by inertia, since  $\text{Re} \gg 1$ . Viscosity plays a small (but crucial) role.
- Turbulent flows are vortical, not irrotational. However, vortical flows need not be turbulent.
- Turbulent flows involve a range of length scales. Vortices exist at both large and small length scales: “Big whorls have little whorls, which feed on their velocity, // And little whorls have lesser whorls, and so on to viscosity.” —Lewis Richardson.

Turbulent flows are unpredictable and simulating them numerically may be difficult as they tend to be numerically unstable. However, it may be possible to predict certain statistics of the flow, such as the behaviour of the mean flow or mean pressure (noting that fluctuations about these means may be great). Some features of turbulence can be shown to be universal, and independent of geometry.

Lewis Richardson’s couplet describes the two processes at work in a turbulent flow. *Vortex stretching* is responsible for creating small vortices out of large ones, while *energy dissipation* causes small vortices to decay.

#### 2.1.2 Vortex stretching

Vortex stretching is the main process by which energy is transferred from large scales to smaller scales.

Taking the curl of the Navier-Stokes equation gives the *vorticity equation*:

$$\frac{\partial \boldsymbol{\omega}}{\partial t} + \mathbf{u} \cdot \nabla \boldsymbol{\omega} = \boldsymbol{\omega} \cdot \nabla \mathbf{u} + \nu \nabla^2 \boldsymbol{\omega} \quad (2.1.1)$$

The second term on the RHS of (2.1.1) means that vorticity is diffused with diffusion constant  $\nu$ . This is a minor effect in flows with  $\text{Re} \gg 1$ . The first term means that when a parcel of fluid is stretched into a column, its vorticity increases and

becomes aligned with the column. Thus stretching a vortex takes energy to a smaller scale. However, if the vortex column is compressed, not nearly as much energy is taken back to the large scale, since the compression in general de-aligns the vorticity vector and the column.

### 2.1.3 Energy dissipation: Kolmogorov's theory (1941)

We know that energy is dissipated in a fluid at a rate

$$\Delta = \int_V \mu |\nabla \mathbf{u}|^2 dV \quad (2.1.2)$$

(or expressed in terms of the strain rate tensor, using  $|\nabla \mathbf{u}|^2 = 2e_{ij}e_{ij}$ ). In a volume with characteristic length  $L$ ,

$$\Delta \sim L^3 |\nabla \mathbf{u}|^2. \quad (2.1.3)$$

For a laminar flow with characteristic velocity  $U$  in a box with sides  $L$ ,  $|\nabla \mathbf{u}| \sim U/L$  and so

$$\Delta \sim \mu \frac{U^2}{L^2} L^3 = \mu U^2 L. \quad (2.1.4)$$

However, for a turbulent flow, the energy dissipation is much faster than this, because the velocity gradients are over much smaller distances, and so  $|\nabla \mathbf{u}| \gg U/L$ .

Although the large-scale structure of the flow might have characteristic lengthscale  $L$ , the small-scale structure of the flow should be described by another lengthscale  $\eta$ , called the *Kolmogorov length scale* or the *Kolmogorov microscale*. This is the lengthscale at which the effects of vortex stretching and dissipation balance each other.

To summarise: The flow is externally driven (continually or initially) at the lengthscale  $L$ , energy cascades to smaller lengthscales by vortex stretching; viscosity acts more and more strongly at these smaller lengthscales. Eventually, energy cascades down to the lengthscale  $\eta$  and proceeds no more.

Let  $\mathbf{U}(\mathbf{k})$  be the Fourier transform of the velocity  $\mathbf{u}(\mathbf{x})$ , using the normalisation

$$\mathbf{U}(\mathbf{k}) = \frac{1}{\sqrt{2\pi}} \int_V \mathbf{u}(\mathbf{x}) e^{-i\mathbf{k} \cdot \mathbf{x}} d\mathbf{x}. \quad (2.1.5)$$

Let

$$E(\mathbf{k}) = \frac{1}{2} \rho \mathbf{U}(\mathbf{k}) \cdot \mathbf{U}(\mathbf{k})^* \quad (2.1.6)$$

be the energy density spectrum. (In defining these Fourier transforms, we are assuming that  $\rho$  is constant and uniform.) The total kinetic energy is

$$KE = \int E(\mathbf{k}) d\mathbf{k} \quad (2.1.7)$$

with the integral taken over wavenumber space. For isotropic turbulence,  $\mathbf{U}$  and  $E$  depend only on the magnitude  $k = |\mathbf{k}|$ .

Since density is constant, we will find it convenient to rewrite the above expressions without  $\rho$ , so that the dimension  $M$  may be set to 1. We therefore work with the energy dissipation rate

$$\epsilon = \int_V \nu |\nabla \mathbf{u}|^2 dV \quad (2.1.8)$$

which has dimensions  $L^2 T^{-3}$ , and with the energy spectrum

$$E(k) = \frac{1}{2} \mathbf{U}(k) \cdot \mathbf{U}(k)^* \quad (2.1.9)$$

which has dimensions  $L^3 T^{-2}$ . We write

$$KE = \int E(k) dk \quad (2.1.10)$$

for the kinetic energy per unit mass, with dimensions  $L^2 T^{-2}$ .

Kolmogorov made two hypotheses about isotropic turbulent flows. These hypotheses allow us to make progress by dimensional analysis, but they do not follow from first principles, and their predictions must be verified experimentally.

**First hypothesis** The rate of dissipation of energy (per unit density),  $\epsilon$  (dimensions  $L^2T^{-3}$ ), depends only on viscosity  $\nu$  (dimensions  $L^2T^{-1}$ ) and on the microscale  $\eta$ . In particular,  $\epsilon$  and  $\eta$  are not to depend on the large lengthscale  $L$ .

By dimensional analysis, this hypothesis allows us to construct  $\eta$  (up to some constant):

$$\eta = (\nu^3/\epsilon)^{1/4} \quad (2.1.11)$$

Note that in a system in dynamic equilibrium, the rate of dissipation of energy is equal to the rate of energy input.<sup>1</sup>

**Second hypothesis** The energy density  $E(k)$  (dimensions  $L^3T^{-2}$ ) depends only on the rate of dissipation  $\epsilon$  and on  $k$  (dimensions  $L^{-1}$ ).

By dimensional analysis,

$$E(k) = C\epsilon^{2/3}k^{-5/3} \quad (2.1.12)$$

for some constant  $C$ .

This second hypothesis is not completely valid. If the flow is in a bounded domain with characteristic lengthscale  $L$ , or if the flow is driven at the lengthscale  $L$ , then the hypothesis is not valid at wavenumbers  $k \sim 1/L$  or below. And the hypothesis is also not valid at small scales with  $k \sim 1/\eta$ , where the details of dissipation start to be important. However, for the range  $1/L \ll k \ll 1/\eta$ , known as the *inertial range*, the hypothesis is justified and is supported by experimental evidence: (2.1.12) is reproduced by experimental data.

## 2.1.4 Two-dimensional turbulence

A turbulent flow in two dimensions is different from one in three dimensions, because in two dimensions the vortex stretching term in (2.1.1) is always zero. Vorticity is conserved, and there is no cascade of energy to smaller lengthscales. Dotting (2.1.1) with  $\boldsymbol{\omega}$  gives us the *enstrophy equation*:

$$\frac{D}{Dt} \left( \frac{1}{2} |\boldsymbol{\omega}|^2 \right) = \nu \left( \nabla^2 \left( \frac{1}{2} |\boldsymbol{\omega}|^2 \right) - |\nabla \boldsymbol{\omega}|^2 \right). \quad (2.1.13)$$

The scalar quantity  $\frac{1}{2} |\boldsymbol{\omega}|^2$  is called the *enstrophy density*.

We obtain a very similar equation for the kinetic energy density by dotting the Navier-Stokes equation with  $\mathbf{u}$ :

$$\frac{D}{Dt} \left( \frac{1}{2} |\mathbf{u}|^2 \right) = \nu \left( \nabla^2 \left( \frac{1}{2} |\mathbf{u}|^2 \right) - |\nabla \mathbf{u}|^2 \right). \quad (2.1.14)$$

Equations 2.1.13 and 2.1.14 tell us that in a 2D flow, enstrophy and kinetic energy are advected, redistributed by diffusion (first term on RHS), and dissipated by viscosity (second term on RHS).

Since total enstrophy (enstrophy density integrated across the volume) must decrease, there must be a net movement of energy to *larger* lengthscales (i.e. smaller  $k$ ). Total enstrophy is proportional to  $\int k^2 E(k) dk$ , so if  $E(k)$  increases at high  $k$ , this increase must be balanced by a greater increase in  $E(k)$  at low  $k$ , so that  $\int k^2 E(k) dk$  never increases.

Hence there is an *anticascade* of energy to larger scales, and a *cascade* of enstrophy to smaller scales.

## 2.2 Simplistic approaches to modelling turbulence

Instead of starting from first principles and trying to solve the Navier-Stokes equations for a turbulent system directly, it is often easier, and more fruitful, to model the effects of turbulence instead.

---

<sup>1</sup>A flow in dynamic equilibrium is unsteady, but it can be characterised by statistics which are constant in time. For example, the mean flow may be zero and the rms velocity may be constant. A turbulent flow may not be in static equilibrium, but it may be in dynamic equilibrium.

### 2.2.1 Molecular diffusion

A direct approach is to model all scales down to the microscale  $\eta = (\nu^3/\epsilon)^{1/4}$ . The energy spectrum (2.1.12) predicts that the kinetic energy per unit volume will be

$$\text{KE density} = \int_{1/L}^{1/\eta} E(k) dk \propto (\epsilon L)^{2/3} \quad (2.2.1)$$

giving a characteristic velocity

$$u \propto \sqrt{\text{KE density}} \propto (\epsilon L)^{1/3} \quad (2.2.2)$$

and therefore a Reynolds number

$$Re = \frac{uL}{\nu} \propto \frac{\epsilon^{1/3} L^{4/3}}{\nu}. \quad (2.2.3)$$

Note that we calculate this Reynolds number using a characteristic velocity calculated only from the turbulent properties, not taking into account any large-scale velocities (such as one driving the flow).

Since  $\eta = (\nu^3/\epsilon)^{1/4}$ , we have

$$Re = \left(\frac{L}{\eta}\right)^{4/3} \gg 1. \quad (2.2.4)$$

For moderately large  $Re$ , direct numerical simulation (DNS) may be possible, but usually  $Re$  is so large that DNS is impractical or impossible.

The problem would be even worse if the fluid were not of uniform and constant density. The mass diffusivity  $\kappa$  and the momentum diffusivity  $\nu$  are compared by the *Schmidt number*  $Sc = \nu/\kappa$ . For salt water,  $Sc \approx 1000$ . In order to simulate the diffusion of mass, we would have to look at an even smaller scale, the *Batchelor scale*  $\lambda_B = \eta/Sc^{1/2}$ .

### 2.2.2 The closure problem

A turbulent flow  $\mathbf{u}$ , and the associated pressure field  $p$ , can be decomposed into its mean part  $\bar{\mathbf{u}}$ , and a fluctuating part  $\mathbf{u}'$  that fluctuates about  $\mathbf{0}$ :  $\bar{\mathbf{u}'} = \mathbf{0}$ . We can model a turbulent flow by ignoring the details of these fluctuations, and looking only at how these fluctuations affect the mean part.<sup>2</sup>

Beginning with the Navier-Stokes equations:

$$\rho \frac{D\mathbf{u}}{Dt} = -\nabla p + \mu \nabla^2 \mathbf{u} + \mathbf{f} \quad (2.2.5)$$

and averaging, we obtain

$$\rho \left( \frac{\partial \bar{\mathbf{u}}}{\partial t} + \bar{\mathbf{u}} \cdot \nabla \bar{\mathbf{u}} \right) = -\nabla \bar{p} + \mu \nabla^2 \bar{\mathbf{u}} + \mathbf{f} - \overline{\rho \mathbf{u}' \cdot \nabla \mathbf{u}'} \quad (2.2.6)$$

(assuming that the body force  $\mathbf{f}$  is a constant). The fluctuations are still present in the quadratic term  $-\overline{\rho \mathbf{u}' \cdot \nabla \mathbf{u}'}$  on the RHS, because (2.2.5) is nonlinear.<sup>3</sup> We cannot remove such terms by more averaging, as that simply introduces further fluctuating terms. This is the *closure problem*: we cannot close the system as we do not know how to deal with these terms. Many approximate closures have been proposed, but none are universally applicable.

Note that

$$-\overline{\rho \mathbf{u}' \cdot \nabla \mathbf{u}'} = -\rho \nabla \cdot (\overline{\mathbf{u}' \mathbf{u}'}) \quad (2.2.7)$$

and so the fluctuations affect the mean flow as though they were an additional stress force, with stress tensor

$$\boldsymbol{\sigma}^{(R)} = -\rho \overline{\mathbf{u}' \mathbf{u}'}. \quad (2.2.8)$$

This ‘stress’ is called the *Reynolds stress*. Different closure models propose different formulae for the Reynolds stresses, usually in terms of some properties of the mean flow.

<sup>2</sup>The mean can be taken as a time average, a local spatial average, or as an ensemble average, but this detail is unimportant for what follows.

<sup>3</sup>If we had a non-constant  $\rho$ , then we would have further such quadratic terms, such as the turbulent buoyancy flux  $\overline{\mathbf{u}' \cdot \nabla \rho}$ .

### 2.2.3 The $k$ - $\epsilon$ model

The most commonly used closure model is the  $k$ - $\epsilon$  model, where  $k = \frac{1}{2} \mathbf{u}' \cdot \mathbf{u}'$  refers to the *turbulent kinetic energy* (per unit density), and  $\epsilon$  to the energy dissipation. The model states that

$$\rho \frac{Dk}{Dt} = \nabla \cdot \left( \frac{\mu_T}{\sigma_k} \nabla k \right) + 2\mu_T \mathbf{S} : \mathbf{S} - \rho\epsilon \quad (2.2.9)$$

where

$$\mu_T = C_\mu \rho \frac{k^2}{\epsilon} \quad (2.2.10)$$

is the *turbulent viscosity*,

$$\mathbf{S} = \frac{1}{2} \left[ \nabla \bar{\mathbf{u}} + (\nabla \bar{\mathbf{u}})^T \right] \quad (2.2.11)$$

is the strain rate tensor corresponding to the mean flow, and  $C_\mu \approx 0.09$  and  $\sigma_k \approx 1.00$  are constants that are determined empirically. Equations 2.2.6 and 2.2.9 together specify the problem for  $\bar{\mathbf{u}}$  completely.

Essentially, the model describes how turbulent kinetic energy is governed. We can interpret (2.2.9) as follows:

- The first term on the RHS represents the diffusion of turbulent kinetic energy, at some (non-constant) rate  $\mu_T/\sigma_k$ .
- The second term represents the generation of turbulent kinetic energy, by means of vortex stretching.
- The third term represents the dissipation of turbulent kinetic energy.

Equation 2.2.9 can be re-written as

$$\rho \frac{D\epsilon}{Dt} = \nabla \cdot \left( \frac{\mu_T}{\sigma_\epsilon} \nabla \epsilon \right) + 2C_{1\epsilon} \frac{\epsilon}{k} \mu_T \mathbf{S} : \mathbf{S} - C_{2\epsilon} \rho \frac{\epsilon^2}{k} \quad (2.2.12)$$

where  $\sigma_\epsilon \approx 1.30$ ,  $C_{1\epsilon} \approx 1.44$  and  $C_{2\epsilon} \approx 1.92$  are constants that are determined empiracally.

Experiments and simulations find that these constants are *universal*.

### 2.2.4 Turbulent diffusion models

As discussed, the vortex stretching process is irreversible and takes energy to smaller lengthscales. There is little back-scatter: smaller lengthscales do not strongly affect the larger scales, except as a sink of energy. This is why we can consider the mean flow as in (2.2.6) and ignore the behaviour of the fluctuations, except as a sink of energy.

This suggests replacing the Reynolds stress with an additional viscosity term that mimics the diffusion of momentum and dissipation of energy without actually describing how this happens. That is, we take

$$-\overline{\mathbf{u}'\mathbf{u}'} = \nu_T \mathbf{S} \quad (2.2.13)$$

where  $\nu_T$  is called the (*turbulent*) *eddy viscosity*. We also write  $\mu_T = \rho\nu_T$ . The force due to Reynolds stresses is therefore

$$\nabla \cdot \boldsymbol{\sigma}^{(R)} = \nabla \cdot \left( -\rho \overline{\mathbf{u}'\mathbf{u}'} \right) \quad (2.2.14)$$

$$= \rho \nabla \cdot (\nu_T \mathbf{S}) \quad (2.2.15)$$

$$= \rho (\nabla \nu_T \cdot \mathbf{S} + \nu_T \nabla \cdot \mathbf{S}) \quad (2.2.16)$$

$$= \rho \left( \nabla \nu_T \cdot \mathbf{S} + \frac{1}{2} \nu_T \nabla^2 \bar{\mathbf{u}} \right). \quad (2.2.17)$$

Putting this into the averaged Navier-Stokes equations gives us

$$\left( \frac{\partial \bar{\mathbf{u}}}{\partial t} + \bar{\mathbf{u}} \cdot \nabla \bar{\mathbf{u}} \right) = -\frac{1}{\rho} \nabla \bar{p} + \left( \nu + \frac{1}{2} \nu_T \right) \nabla^2 \bar{\mathbf{u}} + \frac{1}{\rho} \mathbf{f} + \nabla \nu_T \cdot \mathbf{S}. \quad (2.2.18)$$

Closure models that do this are called *turbulent diffusion models*. Different models propose different expressions for  $\nu_T$ : this is usually not constant, but may depend on the position or on  $\bar{\mathbf{u}}$ .

## 2.2.5 Prandtl's mixing length model

Prandtl's mixing length model is a turbulent diffusion model, in which

$$\nu_T = ku'l \quad (2.2.19)$$

where  $l$  is some *mixing length*,  $u' = \sqrt{|\mathbf{u}'|^2}$  is the *turbulence intensity*, and the *Prandtl ratio*  $k \approx 0.4$  is another empirically-determined constant. The mixing length represents the lengthscale of turbulent eddies; it may vary with position, and depends on the geometry of the problem.

**The law of the wall** For example, in the domain  $z > 0$  bounded by a wall at  $z = 0$ , the lengthscale  $l$  of turbulent eddies is assumed to scale with  $z$ . The turbulence intensity is assumed to be some constant  $q$ . Hence  $\nu_T = kqz$ . The horizontal shear stress is also assumed to be constant.

Assuming that the mean flow is  $\bar{\mathbf{u}} = U(z)\mathbf{e}_x$ , the  $x$ -component of Equation 2.2.18 gives us

$$0 = \frac{1}{\rho}G + \left(\nu + \frac{1}{2}\nu_T\right) \frac{d^2U}{dz^2} + \frac{1}{2}kq \frac{dU}{dz} \quad (2.2.20)$$

where  $G = -\frac{\partial \bar{p}}{\partial x}$  is the horizontal pressure gradient, which is some constant.

In the case  $G = 0$ , we can solve (2.2.20) exactly to give us

$$U(z) = \frac{A}{kq} \log(2\nu + kqz) \quad (2.2.21)$$

where  $A$  is some constant. The condition that shear stress is (approximately) constant allows us to write  $A$  in terms of the *bed shear stress*, the shear stress on  $z = 0$ .

For  $z \ll \frac{\nu}{kq}$ , (2.2.21) says that  $U(z) \propto z$ , as we would expect for a boundary layer. In this region, molecular viscosity  $\nu$  is dominant. However, for larger  $z$ ,  $U(z)$  is logarithmic in  $z$ :

$$U(z) \sim \frac{u_*}{\kappa} \log \frac{z}{z_0} \quad (2.2.22)$$

Equation 2.2.22 is the *law of the wall*. Here  $u_*$  is called the *slip velocity* and  $z_0$  the *roughness height*;  $\kappa \approx 0.41$  is a dimensionless constant called *von Karman's constant*.

In practice, the law of the wall does not hold when  $z$  becomes too large. Far away from the wall, other effects such as small pressure gradients affect the flow, and imperfections in the geometry (such as other walls) may cause the mixing length to stop being  $l \sim z$ . But nonetheless the law is a good approximation for turbulent boundary layers.

## 2.2.6 Entrainment: Diffusion of turbulence

Consider a turbulent patch of length scale  $l$  and turbulence intensity  $u'$ , surrounded by an irrotational flow outside the patch. The vortical motion within the patch will draw in the external fluid, straining and diffusing vorticity into it. Thus the size of the patch will increase; its boundaries move out at a rate proportional to  $u'$ .

This diffusivity of turbulence is called the *turbulent diffusivity*, written  $\kappa_T$ , with  $\kappa_T \sim u'l$ . This is not to be confused with turbulent viscosity, though both are  $\sim u'l$  with similar (but not necessarily equal) constants of proportionality.

This diffusivity of turbulence can explain the growth of the Rayleigh-Taylor instability in a tall tube.

## 2.3 Mixing

### 2.3.1 What is mixing?

Mixing is the blending of fluid particles with different properties, such as density, salinity or temperature. (These properties are related to each other: the density of salt water increases with salinity and decreases with temperature.) There are two processes responsible for mixing:



- *Stirring* is the intermingling of fluid particles of different properties. This produces large gradients in these properties.
- *Diffusion* drives a flux down a gradient that reduces these gradients between adjacent fluid particles.

Diffusion is an irreversible process: there is a ‘preferred’ direction for fluxes, down a gradient; but stirring (on its own) is reversible. Diffusion is a slow process that occurs at the molecular level, whereas stirring can happen quickly and over large lengthscales. Together, stirring and diffusion can cause irreversible mixing very quickly.

In general, a scalar property  $S$  is governed by the advection-diffusion equation

$$\frac{DS}{Dt} = \kappa \nabla^2 S \quad (2.3.1)$$

where  $\kappa$  (dimensions  $L^2 T^{-1}$ ) is the molecular diffusivity of  $S$ . This is often very small: the diffusivity of heat in air is  $\approx 10^{-5} m^2 s^{-1}$  and the diffusivity of salt in water is  $\approx 10^{-9} m^2 s^{-1}$ . The timescale for diffusing across a length  $l$  is therefore  $t \sim l^2 / \kappa$ , which is huge: heat takes a day to diffuse across a metre in air, and salinity takes thirty years to diffuse a metre.

However, stirring (represented by the advection term) can help to create large gradients in  $S$ , which increases the rate of diffusion (by reducing  $l$ ).

### 2.3.2 The energy budget

Consider an incompressible Boussinesq fluid with a linear equation of state.<sup>4</sup> Assume that dissipative heating is unimportant, and ignore any heating effects from dilution, chemical potential energy, and so on.

Begin with the momentum equation for a variable-density fluid:

$$\frac{D(\rho \mathbf{u})}{Dt} = -\nabla p - \rho g \mathbf{e}_z + \rho \nu \nabla^2 \mathbf{u} \quad (2.3.2)$$

and dot with  $\mathbf{u}$ . Since

$$\mathbf{u} \cdot \nabla p = \nabla \cdot (p \mathbf{u}) \quad (2.3.3)$$

for an incompressible fluid, and

$$\mathbf{u} \cdot \rho g \mathbf{e}_z = \frac{D}{Dt}(\rho g z) - \nabla \cdot (g z \kappa \nabla \rho) + g \kappa \frac{\partial \rho}{\partial z} \quad (2.3.4)$$

(where we have used the advection-diffusion equation for  $\rho$ , with mass diffusivity  $\kappa$ ), we have:

$$\frac{D}{Dt} \left( \frac{1}{2} \rho |\mathbf{u}|^2 + \rho g z \right) + \nabla \cdot \left( p \mathbf{u} - \frac{1}{2} \rho \nu \nabla |\mathbf{u}|^2 - g z \kappa \nabla \rho \right) = -g \kappa \frac{\partial \rho}{\partial z} - \rho \nu |\nabla \mathbf{u}|^2. \quad (2.3.5)$$

This equation describes what happens to the kinetic and potential energy density of a fluid. The energy of a parcel of fluid changes due to diffusion, because:

- work is done on it by pressure from neighbouring parcels, causing an energy flux  $p \mathbf{u}$ ;
- viscosity causes the diffusion of kinetic energy, with energy flux  $-\frac{1}{2} \rho \nu \nabla |\mathbf{u}|^2$ ;
- mass diffusion causes the diffusion of potential energy, with energy flux  $-g z \kappa \nabla \rho$ .

The energy of a parcel also changes due to:

- mass diffusion raising the centre of mass, changing the potential energy at a rate  $-g \kappa \frac{\partial \rho}{\partial z}$ ;
- dissipation due to viscosity, decreasing the kinetic energy at a rate  $\rho \nu |\nabla \mathbf{u}|^2$ .

These processes, whose terms appear on the RHS of (2.3.5), are irreversible.

If there are no fluxes of mass or momentum from the boundaries of  $V$ , then integrating the energy equation gives us:

$$\frac{d}{dt}(KE + PE) = W - \epsilon \quad (2.3.6)$$

---

<sup>4</sup>Incompressibility means that  $\nabla \cdot \mathbf{u} = 0$ , but this does not mean that the density  $\rho$  is constant;  $\rho$  is governed by the advection-diffusion equation.

where  $KE = \int_V \frac{1}{2} \rho |\mathbf{u}|^2 dV$  and  $PE = \int_V \rho g z dV$  be the total kinetic and potential energy of the system,  $W = - \int_S p \mathbf{u} \cdot \mathbf{n} dS$  is the rate of pressure working and  $\epsilon = \int_V \rho \nu \nabla^2 |\mathbf{u}|^2 dV$  is the rate of dissipation.

Energy is dissipated into heat. (We are ignoring any effects due to heating.) Kinetic and potential energy can be converted into each other, but mixing and dissipation cause irreversible.

## **2.4 \*Stably stratified flows**

Not covered.

### **2.4.1 Stratification modifies turbulence**

## **2.5 \*Mixing efficiency**

Not covered.

## **2.6 \*Internal mixing**

Not covered.

### **2.6.1 Kelvin-Helmholtz instability**

### **2.6.2 Stratified shear flow**

### **2.6.3 Holmboe instability**

### **2.6.4 Entrainment by internal mixing**



# Chapter 3

## Shallow water

### 3.1 Introduction

### 3.2 Linear waves on an interface

#### 3.2.1 Dispersion relation

#### 3.2.2 Properties of interfacial waves

#### 3.2.3 The short wave limit

#### 3.2.4 The long wave limit

#### 3.2.5 Energy

### 3.3 Shallow water equations

#### 3.3.1 Mathematical definition of ‘shallow’

#### 3.3.2 Derivation from first principles

#### 3.3.3 Boussinesq versus non-Boussinesq

#### 3.3.4 More than one layer

#### 3.3.5 Derivation by averaging

### 3.4 Hyperbolic systems

#### 3.4.1 A model for traffic flow

#### 3.4.2 Shallow water as a hyperbolic system

#### 3.4.3 Matrix formulation

#### 3.4.4 General approach to hyperbolic systems

#### 3.4.5 Implications of hyperbolic nature

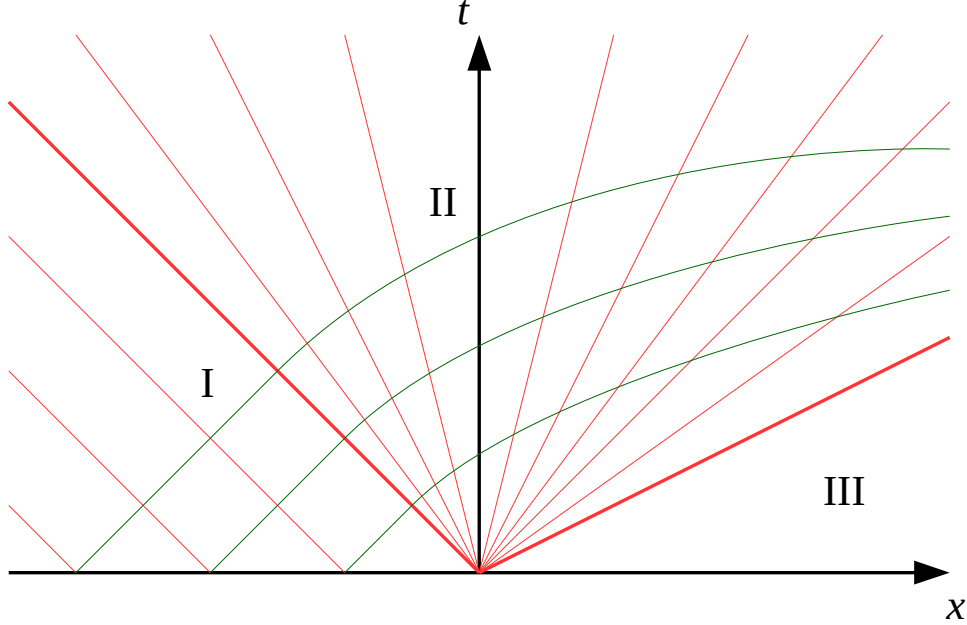


Figure 3.1: Characteristics for the St. Venant solution.

### 3.4.6 The dam break problem

Suppose initially we have  $h = h_0$  in  $x < 0$  and  $h = 0$  in  $x > 0$ , and  $u = 0$  everywhere. What happens?<sup>1</sup> We let  $c = \sqrt{gh}$  and  $c_0 = \sqrt{gh_0}$  for convenience;  $h = c^2/g$ . As before,  $C_{\pm}$  characteristics travel with velocity  $\lambda_{\pm} = u \pm c$  and the quantities  $u \pm 2c$  are constant on  $C_{\pm}$  characteristics respectively.

The characteristics are sketched in Figure 3.1.

In Region I, where  $x < -c_0 t$ , both  $C_-$  and  $C_+$  characteristics come from the region  $x < 0$  at  $t = 0$ , and so  $u = 0$  and  $c = c_0$ .

Assume that the  $C_+$  characteristics from  $x < 0$  fill Region II, the region between  $x = -c_0 t$  and to the left of the front. (We should check that these characteristics do in fact move faster than the front.) Then  $u + 2c = 2c_0$  everywhere in that region. But also  $u - 2c$  is constant along  $C_-$  characteristics. Hence  $u$  and  $c$  must independently be constant along  $C_-$  characteristics. Hence  $C_-$  characteristics have constant slope  $\lambda_- = u - c$ .

If  $X_-$  is the position of a  $C_-$  characteristic, then

$$\frac{dX_-}{dt} = u - c. \quad (3.4.1)$$

So  $C_-$  characteristics which start at the origin are given by

$$\frac{x}{t} = u - c. \quad (3.4.2)$$

<sup>1</sup>The following discussion is largely based on the discussion at [http://www.wikiwaves.org/Nonlinear\\_Shallow\\_Water\\_Waves](http://www.wikiwaves.org/Nonlinear_Shallow_Water_Waves)

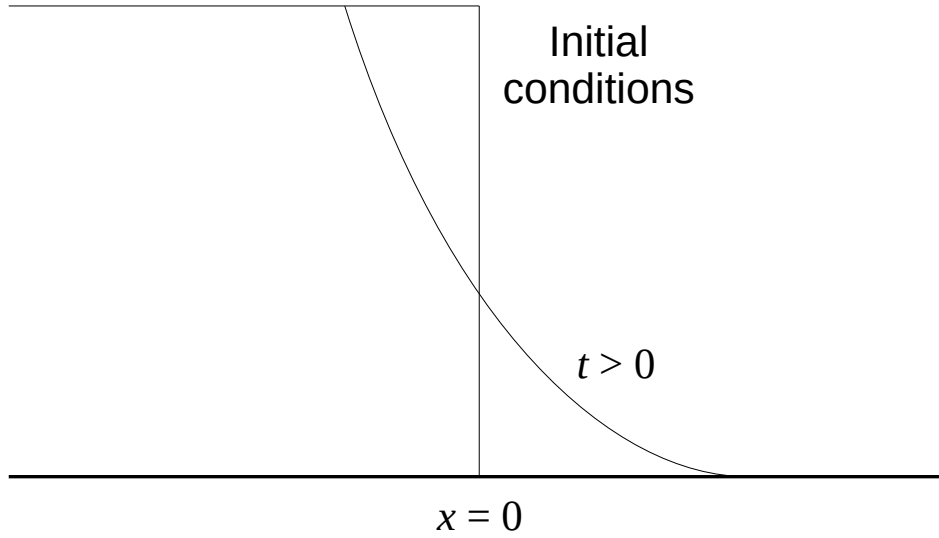


Figure 3.2: The St. Venant solution.

We solve (3.4.2) together with  $u + 2c = 2c_0$  to solve for  $u$  and  $c$ :

$$u = \frac{2}{3} \left( c_0 + \frac{x}{t} \right) \quad (3.4.3)$$

$$c = \frac{1}{3} \left( 2c_0 - \frac{x}{t} \right) \quad (3.4.4)$$

$$h = \frac{1}{9g} \left( 2c_0 - \frac{x}{t} \right)^2. \quad (3.4.5)$$

In particular,  $h = 0$  at  $x = 2c_0 t$ , so the front moves at speed  $2c_0$ . On the other hand,

$$\lambda_+ = u + c \quad (3.4.6)$$

$$= \frac{4}{3} c_0 + \frac{x}{3t} \quad (3.4.7)$$

$$(3.4.8)$$

is the speed at which the  $C_+$  characteristics move.

This is called the St. Venant solution, and it is sketched in Figure 3.2. It is not observed in practice. In practice, *bottom drag* and *form drag* have important effects which resist motion. Bottom drag is significant if the current is much more dense than the ambient. Form drag is significant if the ambient is much more dense than the current, or if the density difference is small.

### 3.4.7 Entrainment into shallow water flows

Turbulent often produces mixing: the blending of fluid particles of a different character. If we have a turbulent shallow water flow, then not only does the turbulence transport momentum within the flow, but it can also drive mixing between

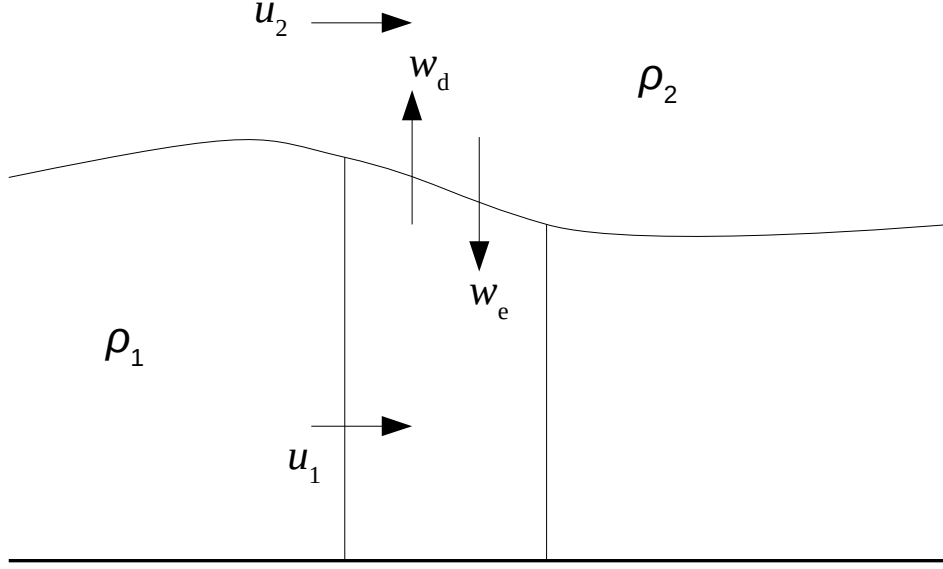


Figure 3.3: Schematic for entrainment/detrainment for a shallow layer.

the flow and the ambient fluid. In particular, if the turbulence is in the moving shallow water layer, then it can cause the layer to entrain ambient fluid into the layer, affecting its volume, density and possibly its momentum.

This is true for *miscible fluids*. Immiscible fluids can entrain each other, but the resulting two-phase flow will separate again if allowed to.

Shallow water flows may be unstable both to short wave instabilities, such as Kelvin-Helmholtz and Holmboe instabilities, and to long wave instabilities.

Entrainment reduces the density contrast and therefore reduces  $g'$ . It also increases the volume of the layer of fluid, so increases  $h$ . For a quiescent ambient, the result of entrainment is that  $g'h$  is conserved. Also, the fluid that is being drawn in has a different (zero) momentum.

The setup is sketched in Figure 3.3. Assume that the ambient fluid density  $\rho_2$  is constant, so that only the density in the layer  $\rho_1$  changes. Let  $w_e$  be the speed of entrainment and  $w_d$  the speed of ‘detrainment’. Then, by considering fluxes in and out of a control volume:

- Conservation of volume gives

$$\frac{\partial h}{\partial t} + \frac{\partial}{\partial x} (u_1 h) = w_e - w_d. \quad (3.4.9)$$

- Conservation of mass gives

$$\frac{\partial}{\partial t} (\rho_1 h) + \frac{\partial}{\partial x} (u_1 \rho_1 h) = w_e \rho_2 - w_d \rho_1 \quad (3.4.10)$$

or, using conservation of volume,

$$\frac{\partial \rho_1}{\partial t} + u_1 \frac{\partial \rho_1 h}{\partial x} = -\frac{w_e}{h} (\rho_1 - \rho_2) \quad (3.4.11)$$

- The momentum balance (ignoring drag) gives

$$\frac{\partial}{\partial t} (\rho_1 h u_1) + \frac{\partial}{\partial x} \left( u_1 \rho_1 h u_1 + \frac{1}{2} (\rho_1 - \rho_2) g h^2 \right) = w_e \rho_2 u_2 - w_d \rho_1 u_1. \quad (3.4.12)$$

We get this by taking the pressure to be hydrostatic and equal to  $p_0$  at some reference height  $z_0$ . Then the horizontal pressure gradient, integrated over the horizontal cross section, is

$$\int_0^h \frac{\partial p}{\partial x} dz = \int_0^h \frac{\partial}{\partial x} (p_0 + \rho_2 g(z_0 - z) + (\rho_1 - \rho_2)g(h - z)) dz \quad (3.4.13)$$

$$= \dots \quad (3.4.14)$$

$$= \frac{\partial}{\partial x} \left( \frac{1}{2} g(\rho_1 - \rho_2) h^2 \right). \quad (3.4.15)$$

Using conservation of mass, the momentum equation can also be written as

$$\frac{\partial u_1}{\partial t} + u_1 \frac{\partial u_1}{\partial t} + g \frac{\rho_1 - \rho_2}{\rho_1} \frac{\partial h}{\partial x} + \frac{gh}{2\rho_1} \frac{\partial}{\partial x} (\rho_1 - \rho_2) = -w_e \frac{\rho_2}{\rho_1} \frac{u_1 - u_2}{h} \quad (3.4.16)$$

Note that conservation of volume does not strictly hold: Mass is conserved, but the density of a mixture will be different from the density of its constituents. For ‘linear mixing’, we can ignore changes in volume. We work in the Boussinesq approximation where  $\rho_{1,2}$  are approximately equal, and assume that the ambient fluid is stationary:  $u_2 = 0$ . Then (3.4.16) reduces to

$$\frac{\partial u_1}{\partial t} + u_1 \frac{\partial u_1}{\partial t} + g' \frac{\partial h}{\partial x} + \frac{h}{2} \frac{\partial g'}{\partial x} = -w_e \frac{u_1}{h} \quad (3.4.17)$$

where  $g' = g(\rho_1 - \rho_2)/\rho$ . If we also write (3.4.11) in terms of  $g'$ , then

$$\frac{\partial g'}{\partial t} + u_1 \frac{\partial g'}{\partial x} = -g' \frac{w_e}{h} \quad (3.4.18)$$

$$\frac{\partial h}{\partial t} + u_1 \frac{\partial h}{\partial x} + h \frac{\partial u_1}{\partial x} = w_e - w_d \quad (3.4.19)$$

$$\frac{\partial u_1}{\partial t} + \frac{h}{2} \frac{\partial g'}{\partial x} + g' \frac{\partial h}{\partial x} + u_1 \frac{\partial u_1}{\partial x} = -u_1 \frac{w_e}{h} \quad (3.4.20)$$

or, in matrix form,

$$\begin{pmatrix} u_1 & 0 & 0 \\ 0 & u_1 & h \\ \frac{h}{2} & g' & u_1 \end{pmatrix} \begin{pmatrix} g' \\ h \\ u_1 \end{pmatrix}_x + \begin{pmatrix} g' \\ h \\ u_1 \end{pmatrix}_t = \begin{pmatrix} -g' \frac{w_e}{h} \\ w_e - w_d \\ -u_1 \frac{w_e}{h} \end{pmatrix}. \quad (3.4.21)$$

The system is still hyperbolic, as the matrix still admits three real, distinct eigenvalues:  $\lambda = u_1$  and  $\lambda = u_1 \pm (g'h)^{1/2}$ . The latter two represent interfacial waves as before; the characteristic with  $\lambda = u_1$  represents the advection of density. Since the RHS of (3.4.21) is nonzero, the evolution equations along those characteristics are inhomogeneous:

- Along the  $\lambda = u_1$  characteristic, we have

$$\frac{\partial g'}{\partial s} = -g' \frac{w_e}{h}; \quad (3.4.22)$$

- along the  $\lambda = u_1 + (g'h)^{1/2}$  characteristic,

$$\frac{h}{2\sqrt{g'}} \frac{\partial g'}{\partial s} + \sqrt{g'} \frac{\partial h}{\partial s} + \sqrt{h} \frac{\partial u_1}{\partial s} = -\frac{1}{2} \sqrt{g'} w_e + \sqrt{g'} (w_e + w_d) - u_1 \frac{w_e}{\sqrt{h}}. \quad (3.4.23)$$



## 3.5 Gravity currents

### 3.5.1 A moving dam problem

### 3.5.2 Description

### 3.5.3 Early models

### 3.5.4 Cavity flows

### 3.5.5 \*Morden and Beiburg

### 3.5.6 Gravity currents and characteristics

### 3.5.7 Modelling gravity currents

### 3.5.8 Real life is more complex



## Chapter 4

# Jets, plumes and thermals

A *jet* is a continuous directed release of fluid with a specified momentum from an isolated source (such as blowing from lips). A *plume* is a continuous release of buoyant fluid from an isolated source, with, ideally, no mass or momentum flux (e.g. a candle). The direction of a plume is given by  $\mathbf{g}$ . A *thermal* is an isolated release of a finite patch of buoyancy.

Note that ‘continuous’, ‘stable’ and ‘steady’ are distinct terms, and no one of them implies either of the other.

We will assume that jets and plumes are axisymmetric and self-similar, so that any averaged quantity  $\bar{\phi}$  can be written as

$$\bar{\phi} = \Phi(z)f(r/b) \quad (4.0.1)$$

where  $b$  is the ‘radius’ of the plume. The averaging may be an ensemble average or a temporal average. Specific forms for the function  $f$  may be taken. The simplest form for  $f$  is the *top-hat* profile

$$f(x) = \begin{cases} 0 & \text{if } x > 1 \\ 1 & \text{if } x < 1. \end{cases} \quad (4.0.2)$$

Other forms, such as the Gaussian  $f(x) = \exp(-x^2)$ , may also be used.

### 4.1 Jets

We define

$$\pi Q = \frac{1}{T} \int_0^T \int_0^\infty \int_{-\pi}^\pi w r \, d\theta \, dr \, dt \quad (4.1.1)$$

$$\pi M = \frac{1}{T} \int_0^T \int_0^\infty \int_{-\pi}^\pi w^2 r \, d\theta \, dr \, dt \quad (4.1.2)$$

$$(4.1.3)$$

as, respectively, the volume flux and momentum flux divided by density. The integral over  $t$  enacts a time-averaging. The  $\pi$ ’s on the LHS are for convenience. For a top hat profile, these become

$$\pi Q = \pi b^2 W \quad (4.1.4)$$

$$\pi M = \pi b^2 W^2 \quad (4.1.5)$$

where we write  $W$  instead of  $w$  to emphasise that this is an averaged velocity, reserving  $w$  for the fluctuating local velocity. We have

$$W = M/Q \quad (4.1.6)$$

$$b = Q/M^{1/2} \quad (4.1.7)$$

Consider a steady jet travelling in the  $z$  direction. As the fluid in the jet travels, it entrains the surrounding fluid with entrainment velocity  $u_e$ . Experiments find that

$$u_e = \alpha W \quad (4.1.8)$$

where the entrainment coefficient  $\alpha$  is between 0.065 and 0.080 for a top hat profile. Thus, the volume flux satisfies

$$\pi \frac{dQ}{dz} = 2\pi b u_e \quad (4.1.9)$$

$$= 2\pi b \alpha W \quad (4.1.10)$$

$$= 2\alpha \pi M^{1/2}. \quad (4.1.11)$$

Meanwhile, conservation of momentum gives

$$\pi \frac{dM}{dz} = 0. \quad (4.1.12)$$

Hence  $M = M_0$  is constant along the plume. This gives

$$Q = 2\alpha M_0^{1/2} (z + z_\nu) \quad (4.1.13)$$

$$b = \alpha (z + z_\nu) \quad (4.1.14)$$

$$W = \frac{M_0^{1/2}}{2\alpha (z + z_\nu)}. \quad (4.1.15)$$

So, the jet's thickness increases linearly with  $z$ , and the fluid velocity decreases with  $z$ . The point  $z = -z_\nu$  is the 'virtual origin' of the jet: it looks as though there is a point source of momentum at this point, even though boundary conditions are being specified at  $z = 0$ .

## 4.2 General plume equations

### 4.2.1 Self-similar plumes

For plumes, the density of the fluid is not homogeneous, and so we need to consider fluxes of mass and momentum, rather than fluxes of volume and  $\frac{\text{momentum}}{\text{density}}$ . Therefore, we define

$$\pi Q = \frac{1}{T} \int_0^T \int_0^\infty \int_{-\pi}^\pi \hat{\rho} w r \, d\theta \, dr \, dt \quad (4.2.1)$$

$$\pi M = \frac{1}{T} \int_0^T \int_0^\infty \int_{-\pi}^\pi \hat{\rho} w^2 r \, d\theta \, dr \, dt \quad (4.2.2)$$

$$(4.2.3)$$

as the mass flux and momentum flux respectively. We also define

$$\pi F = \frac{1}{T} \int_0^T \int_0^\infty \int_{-\pi}^\pi (\rho_0 - \hat{\rho}) g w r \, d\theta \, dr \, dt \quad (4.2.4)$$

as the buoyancy flux. Here  $\hat{\rho}$  is the instantaneous, fluctuating density inside the plume, and  $\rho_0$  is the density of the surrounding fluid. For top-hat profiles, these become

$$\pi Q = \pi \rho b^2 W \quad (4.2.5)$$

$$\pi M = \pi \rho b^2 W^2 \quad (4.2.6)$$

$$\pi F = \pi (\rho_0 - \rho) g b^2 W \quad (4.2.7)$$

where  $\rho$  is the density in the plume averaged across a cross-section. We also have

$$W = M/Q \quad (4.2.8)$$

$$b = Q/(\rho M)^{1/2} \quad (4.2.9)$$

$$g' = F/Q. \quad (4.2.10)$$

## 4.2.2 Time-dependent plume equations

Volume, mass and momentum balances on the plume give

$$\frac{\partial}{\partial t} (\pi b^2) + \frac{\partial}{\partial z} (\pi b^2 W) = 2\pi b u_e \quad (4.2.11)$$

$$\frac{\partial}{\partial t} (\pi \rho b^2) + \frac{\partial}{\partial z} (\pi \rho b^2 W) = 2\pi \rho_0 b u_e \quad (4.2.12)$$

$$\frac{\partial}{\partial t} (\pi \rho b^2 W) + \frac{\partial}{\partial z} (\pi \rho b^2 W^2) = \pi b^2 (\rho_0 - \rho) g \quad (4.2.13)$$

$$(4.2.14)$$

which can also be written as

$$\frac{\partial}{\partial t} (\pi b^2) + \frac{\partial}{\partial z} (\pi b^2 W) = 2\pi b u_e \quad (4.2.15)$$

$$\frac{\partial \rho}{\partial t} + W \frac{\partial \rho}{\partial z} = \frac{2(\rho_0 - \rho) u_e}{b} \quad (4.2.16)$$

$$\frac{\partial W}{\partial t} + W \frac{\partial W}{\partial z} = \frac{g(\rho_0 - \rho)}{\rho} - 2 \frac{\rho_0}{\rho} \frac{u_e W}{b} \quad (4.2.17)$$

Experiments show that the entrainment velocity for plumes is

$$u_e = \alpha \left( \frac{\rho}{\rho_0} \right)^{1/2} W \quad (4.2.18)$$

where  $\alpha$  is between 0.1 and 0.16 (but again depends on the top-hat profile). For Boussinesq plumes,  $\rho \sim \rho_0$  and so  $u_e \sim \alpha W$ .

It can be shown that, in the Boussinesq case, the system is not hyperbolic, but is parabolic, and admits similarity solutions, as expected.

## 4.3 Plumes in a homogeneous environment

### 4.3.1 Steady Boussinesq plumes

It is found that  $F$  is constant.

### 4.3.2 Time-dependent plumes

### 4.3.3 Steady non-Boussinesq plumes

## 4.4 Plumes in a stratified environment

Now the ambient density  $\rho_0$  is a function of height. This must be accounted for in the equation for  $F$ . It is found that  $F$  is not constant, and a power-law solution does not exist.

4.4.1 Rise height

4.4.2 Series solution in Boussinesq fluid

4.5 \*Thermal in a homogeneous environment

4.6 \*Thermals in a stratified environment

## Chapter 5

# Buoyancy-driven flows





## Chapter 6

# Particle-laden and granular flow

### 6.1 Types of particulate flows

Models for particulate flows are ad-hoc and apply to different geophysical situations, depending on which assumptions may be made about the flows and the particles:

**Grain suspension by fluid turbulence** Examples include pyroclastic flows<sup>1</sup>, turbidity currents<sup>2</sup> and powder snow<sup>3</sup>. In such flows, the particles may be very concentrated and denser than the fluid, but they are kept in suspension by the turbulent flow of the fluid; any particles which settle quickly undergo *resuspension*.

**Liquefied and fluidised flow** Examples include dense snow avalanches and *some* mudflows. In these cases, the flow is dominant and the particles move with the flow; in this regime, particles do not interact with each other (*cohesionlessness*), as they are separated from each other (*grain dispersion*). Their effect is to increase the viscosity of the fluid. However, this limits the possibility of turbulence, and so particles can settle out at the base of the fluid.

**Dry grain flow and interactions** Examples include sand dune avalanches and rock slides. Now the particles interact with each other, colliding frequently; the fluid acts as a lubricant.

**Grain-supported matrix** Examples include debris flows and lahars, or large boulders suspended in a muddy matrix. Now cohesion has a large rôle to play. The flow of mud and slurries are non-Newtonian. Effects of cohesion, friction, pore pressure, etc. may be modelled using other stress-shear rate relationships (*rheological models*), including power laws, Bingham plastic models and Herschel-Bulkley models. In the latter two models, the fluid has a *yield strength*: a minimum shear stress must be applied before any flow occurs.

---

<sup>1</sup>Wikipedia: A pyroclastic flow is a fast-moving current of hot gas and rock (collectively known as tephra), which reaches speeds moving away from a volcano of up to 700 km/h (450 mph). The gas can reach temperatures of about 1,000 °C. Pyroclastic flows normally hug the ground and travel downhill, or spread laterally under gravity. Their speed depends upon the density of the current, the volcanic output rate, and the gradient of the slope. They are a common and devastating result of certain explosive volcanic eruptions.

<sup>2</sup>Wikipedia: A turbidity current is a current of rapidly moving, sediment-laden water moving down a slope through water, or another fluid. The current moves because it has a higher density than the fluid through which it flows—the driving force of a turbidity current derives from its sediment, which renders the turbid water denser than the clear water above. The deposit of a turbidity current is called a turbidite.

<sup>3</sup>Wikipedia: Freshly fallen, uncompacted snow. The density and moisture content of powder snow can vary widely; snowfall in coastal regions and areas with higher humidity is usually heavier than a similar depth of snowfall in an arid or continental region. Light, dry (low moisture content, typically 4–7% water content) powder snow is prized by skiers and snowboarders. It is often found in the Rocky Mountains of North America and in most regions in Japan.

## 6.2 Physics within a particle gravity current

A particle gravity current can be modelled as having a main body and a base. In the main body, there is a well-mixed suspension of particles in a turbulent flow; in the base, the particles and fluid have low velocity and particles are settling out.

We consider the flow of a current consisting of a fluid with a well-mixed suspension of particles, with the particles denser than the fluid. The difference in density means that *buoyancy* has a role to play. The flow is driven by a pressure gradient and affected by the effects of buoyancy. Viscosity is negligible, so buoyancy and inertia balance each other.

Particles can settle out of suspension (*sedimentation*) or be *entrained* into suspension. This means the concentration of the particles in the suspension changes. So the density difference between the suspension and the ambient fluid changes too.

Let

- $\rho_0$  denote the density of the fluid;
- $\mu_0$  denote the viscosity of the fluid;
- $\rho_p$  denote the density of the particles;
- $\phi$  denote the concentration of particles.

Then the *bulk density* of the fluid-particle mixture is

$$\rho_l = \rho_0 + \phi(\rho_p - \rho_0) \quad (6.2.1)$$

and the *reduced gravity* is

$$g' = g \frac{\rho_l - \rho_0}{\rho_0} = \phi g \frac{\rho_p - \rho_0}{\rho_0} = \phi g'_0 \quad (6.2.2)$$

where

$$g'_0 = g \frac{\rho_p - \rho_0}{\rho_0}. \quad (6.2.3)$$

## 6.3 Sedimenting particle-laden flows

We assume that particles are small compared to the scale of motion, so that the presence of an individual particle has a negligible effect on the bulk flow. However, the collective of particles will have an effect. We also assume that particles sediment slowly, over a timescale much larger than that of the flow; and that particles are numerous and well-mixed, so that we can talk of the ‘concentration’ of particles, rather than having to study individual particles.

Note that although we use the word ‘particles’, all of this theory could just as well apply to bubbles or to droplets; a bubble can be regarded as a particle with density negligible compared to that of the fluid; the reduced gravity is negative.

The suspension changes the bulk properties of the fluid. As discussed, the suspension has density

$$\rho_l = \rho_0 + \phi(\rho_p - \rho_0) \quad (6.3.1)$$

where  $\phi$  is the concentration by volume. We model the viscosity of the suspension as having a power law dependence on the concentration:

$$\mu = \mu_0 \left(1 - \frac{\phi}{\phi_{max}}\right)^{-n\phi_{max}} \quad (6.3.2)$$

where  $\phi_{max}$  is the maximum suspension concentration that can be supported. For spherical particles,  $n = \frac{5}{2}$ .<sup>4</sup>

We define the *particle Reynolds number*

$$\text{Re}_p = \frac{\rho_l D u_s}{\mu} \quad (6.3.3)$$

which governs many properties of the flow. Here  $D$  is the diameter of a particle, and  $u_s$  is the settling velocity, which we will determine.

---

<sup>4</sup>A similar result is derived in a *Slow Viscous Flow* past examination question, 2013/68/1.

When particles sediment out of suspension, we are left with a *clarified* fluid, devoid of particles, and a concentrated suspension at the bottom where all the particles gather.

Sedimenting flows can exhibit four types of behaviour, depending on  $\text{Re}_p$  and on the concentration  $\phi$ :

- Type I: Free settling of individual particles
- Type II: Flocculant settling: Coalescence of particles
- Type III: Hindered (zone) settling: Restricted, fluid motion
- Type IV: Compression settling: Mechanical support

We will discuss Types I and III in detail. Types II and IV involve complicated particle-particle interactions.

### 6.3.1 Type I: Free settling of individual particles

This occurs when particles are very well-separated from each other, and so do not interact with each other. This occurs at very low concentrations (the *dilute limit*).

**The particle Reynolds number** When a sphere of diameter  $D$  moves at a speed  $u_s$  through otherwise unmoving fluid, its behaviour depends on the particle Reynolds number  $\text{Re}_p = \frac{\rho_l D u_s}{\mu}$ . If  $\text{Re}_p \ll 1$  then the flow past the sphere is *laminar*; the sphere travels smoothly. But if  $10^3 \ll \text{Re}_p \ll 2 \cdot 10^5$  then the flow is in the *inertial regime*; the sphere travels roughly, and the boundary layer on the sphere is turbulent. Various other regimes are possible for different values of  $\text{Re}_p$ ; they are discussed in Middleton and Southard (1984).

**The drag coefficient** By dimensional analysis, the drag  $F_D$  on a particle travelling at  $u_s$  through a fluid is

$$F_D = C_D \frac{1}{2} \rho_l u_s^2 A_p \quad (6.3.4)$$

where  $A_p$  is the planar area of the particle. (See Prandtl and Tietjens, 1957 for details.) The dimensionless coefficient  $C_D$  is called the *drag coefficient*, and depends on the Reynolds number. The dependence may be found empirically:

- When  $\text{Re}_p \ll 1$ , then  $C_D$  is inversely proportional to  $\text{Re}_p$ :

$$C_D = \frac{24}{\text{Re}_p} \quad (6.3.5)$$

- When  $0.2 < \text{Re}_p < 10^3$ , there is a transitional region.
- When  $10^3 < \text{Re}_p < 2 \cdot 10^5$ ,  $C_D$  is approximately constant for cylinders, spheres and discs. For these shapes,  $C_D \approx 0.44$ .
- At  $\text{Re}_p \approx 2 \cdot 10^5$ , the drag coefficient drops very quickly before increasing much more slowly again. This is called the *drag crisis regime*, and arises because of a flow separation.

**The settling velocity** So what is the settling velocity  $u_s$ ? We consider the momentum balance on a particle in suspension. The forces acting on the particle are drag, buoyancy and gravity, and so:

$$m \frac{du}{dt} = F_g - F_b - F_D \quad (6.3.6)$$

$$F_D = C_D \frac{1}{2} \rho_l u^2 A_p \quad (6.3.7)$$

$$F_b = \rho_l g V \quad (6.3.8)$$

$$F_g = \rho_p g V \quad (6.3.9)$$

where  $V$  is the volume of the particle. The expression for  $F_b$  is given by Archimedes' law: the buoyancy force is  $g$  times the mass of fluid displaced. (Note that the fluid displaced is said to have density  $\rho_l$  rather than  $\rho_0$ , though the two are

approximately equal in the dilute limit.) Setting  $\frac{du}{dt} = 0$  and solving for  $u$  gives us the terminal velocity, which is the settling velocity.

For a sphere of diameter  $D$ , we have  $V = \frac{1}{6}\pi D^3$  and  $A_p = \frac{1}{4}\pi D^2$ , and so

$$u_s = \sqrt{\frac{4g(\rho_p - \rho_l)D}{3C_D\rho_l}}. \quad (6.3.10)$$

Recall that in the Stokes regime with  $\text{Re}_p < 0.2$ , we have  $C_D = \frac{24}{\text{Re}_p}$ . Hence:

$$F_D = 3\pi u_s \mu D \quad (6.3.11)$$

$$u_s = \frac{g(\rho_p - \rho_l)D^2}{18\mu} \quad (6.3.12)$$

with  $u_s \propto D^2$  and dependent on  $\mu$ . But in the inertial, turbulent regime, with  $10^3 < \text{Re}_p < 2 \cdot 10^5$ , we have  $C_D = 0.44$  constant, and

$$F_D = 0.055\pi\rho_l u_s^2 D^2 \quad (6.3.13)$$

$$u_s = 1.74 \sqrt{\frac{g(\rho_p - \rho_l)D}{\rho_l}} \quad (6.3.14)$$

with  $u_s \propto D^{1/2}$  and not dependent on  $\mu$ .

These predictions are confirmed by observations: the Stokes regime holds for fine grains such as silt, whereas the inertial regime holds for very coarse sand, granules and pebbles (provided that particle-particle interactions may be neglected). However, for  $D$  between 0.1mm and 1mm (such as for medium or coarse sand), we are in the transitional regime where neither the Stokes nor the turbulent predictions hold well. Many equations have been proposed to describe the intermediate region, including the *Ferguson-Church equation*.<sup>5</sup>

**Advection and diffusion of particles** The concentration of particles  $\phi$  is governed by an advection-diffusion equation:

$$\frac{\partial \phi}{\partial t} + \mathbf{u} \cdot \nabla \phi = D \nabla^2 \phi \quad (6.3.15)$$

where  $D$  now denotes the diffusion coefficient, *not* the particle diameter. The settling velocity which we have so far calculated was for an otherwise stationary fluid, so in (6.3.15) the particle velocity  $\mathbf{u}$  is equal to

$$\mathbf{u} = (u, v, w) + (0, 0, -u_s) \quad (6.3.16)$$

where  $(u, v, w)$  is the mean velocity of the fluid.<sup>6</sup>

If there is no mean background fluid flow, then (6.3.15) reduces to

$$\frac{\partial \phi}{\partial t} - u_s \frac{\partial \phi}{\partial z} = D \nabla^2 \phi. \quad (6.3.17)$$

If we neglect dependencies on  $x$  and  $y$ , then (6.3.17) is Burgers' equation.

The diffusion coefficient  $D$  depends on  $\text{Re}_p$  and whether the flow is laminar or turbulent. In the laminar regime, diffusion of particles is due to molecular (Brownian) diffusion:

$$D = D_B \sim \frac{kT}{6\pi\mu r} \quad (6.3.18)$$

where  $r$  is the radius of particles,  $k$  is the Boltzmann constant and  $T$  is the temperature. Molecular diffusion is a very slow process unless  $r$  is very small, such as for aerosol particles.

<sup>5</sup>See <http://hinderedsettling.com/2013/08/09/grain-settling-python/>.

<sup>6</sup>We can have fluid flow even if there is no mean fluid flow, if we are in a turbulent regime.

However, in the turbulent regime, diffusion of particles is due to turbulent diffusivity:

$$D = D_T \sim u^* h \quad (6.3.19)$$

where  $u^* = \sqrt{\frac{\tau_b}{\rho}}$  is the shear velocity (friction velocity),  $\tau_b$  is the shear stress at the bottom, and  $h$  is some turbulence length scale, such as the distance from the bottom.

Note that if we ignore diffusivity in Equation 6.3.17 and set  $D = 0$ , then the resulting equation admits shocks. This is because when the diffusivity is small, we have fronts where the concentration changes very sharply. To calculate the speed at which these fronts move, we can use the Rankine-Hugoniot conditions.

### 6.3.2 Type II: Flocculent settling, particle coalescence

In this regime, particles may coalesce together to form larger particles, which have larger settling velocities. Therefore settling in this regime occurs quicker than if particles do not coalesce. There is no mathematical theory to model this regime.

### 6.3.3 Type III: Hindered (zone) settling

When there are many particles, then particles no longer settle at the  $u_s$  which we have calculated, but at some slower velocity  $u_h$ , a *hindered settling velocity*. The hindered settling velocity depends on  $\phi$  and on  $u_s$ . As  $\phi$  increases,  $u_h$  decreases. As  $\phi$  approaches  $\phi_{max}$ , then more complicated inter-particle interactions take place and we start to have compression settling.

The model that we will use is

$$u_h = u_s \left(1 - \frac{\phi}{\phi_{max}}\right)^\alpha \quad (6.3.20)$$

where  $\alpha$  is some empirically determined constant which depends on the flow regime.<sup>7</sup> Richardson and Zaki (1954) found that for  $\phi$  up to 0.35,  $\alpha = 4.65$  in the laminar regime  $Re_p < 0.2$  and  $\alpha = 2.39$  in the regime  $Re_p > 500$ .

The settling flux is

$$Q_h = u_h \phi. \quad (6.3.21)$$

In a suspension with a steady concentration profile  $\phi(z)$ , the settling flux of particles downwards is balanced by diffusive flux upwards. Thus the concentration satisfies the *Rouse equation*:

$$\phi(z)u_h(z) = -D \frac{d\phi(z)}{dz} \quad (6.3.22)$$

where  $D$  is a diffusivity. This tends to happen if the flow is turbulent and  $D$  is large.

**Nonlinear kinematic wave equation** If  $\phi = \phi(z, t)$  and diffusivity is small (which happens if the flow is laminar) then, as we have seen before,  $\phi$  obeys the ‘traffic equation’

$$\frac{\partial \phi}{\partial t} + \frac{\partial \phi u_h}{\partial z} = 0 \quad (6.3.23)$$

which may be solved by the method of characteristics. Again, solutions to this equation have shocks, which represent sharp fronts in a settling suspension.

### Settling of particles on inclines

### 6.3.4 Type IV: Compressional settling, compacting

This regime occurs in regions of very high concentration. Stirring or tapping can allow the liquid to escape. The packing fraction may increase locally, leading to increased stability.

---

<sup>7</sup>Following ‘A physical introduction to suspension dynamics’.

## 6.4 Modelling a particulate gravity current

See [1] for more details and more complicated models.

### 6.4.1 A simple box model

We assume a ‘box profile’ for the particulate gravity current: it has a length  $L(t)$  and a constant height  $h(t)$  throughout its length, except possibly at its nose, where the nose height  $h_N$  may be larger than  $h$ . We let  $u$  be the velocity in the current, and  $u_N$  be the velocity of the nose. The nose velocity is related to  $L$  by  $\frac{dL}{dt} = u_N$ . For simplicity we will take  $h_N = h$  and  $u_N = u$ . We will also assume that the particle concentration  $\phi$  is uniform throughout the current, and that particles are settling with settling velocity  $u_s$ .

Throughout, we assume that  $\phi \ll 1$ , so that the settling is unhindered, and the current is Boussinesq.

Let  $\rho_0$  be the fluid density, and  $\rho_p$  be the particle density. Then the density of the current, with concentration  $\phi$ , is  $\rho_l = (1 - \phi)\rho_0 + \phi\rho_p$ . We define a reduced gravity

$$g' = g \frac{\rho_l - \rho_0}{\rho_0} = g\phi \frac{\rho_p - \rho_0}{\rho_0} = \phi g_0'. \quad (6.4.1)$$

Since the current is Boussinesq,  $g' \ll g$ .

Assume that there is no entrainment. Then the volume of the current is constant, and so the mass of the current  $M = L(t)h(t)$  is constant. Hence particle conservation gives

$$\frac{d(M\phi)}{dt} = M \frac{d\phi}{dt} = -u_s \phi(t)L(t) \quad (6.4.2)$$

Hence,

$$\frac{d\phi}{dt} = -\frac{u_s \phi}{h}. \quad (6.4.3)$$

Meanwhile, the value of  $u_N = \frac{dL}{dt}$  is related to the nose height  $h_N$  by a Froude number condition

$$u_N = \frac{dL}{dt} = \text{Fr}_f (\phi g_0' h_N)^{1/2} \quad (6.4.4)$$

where  $\text{Fr}_f$  is the front Froude number. For an ideal fluid with irrotational flow, Bernoulli’s theorem would predict that  $\text{Fr}_f = \sqrt{2}$ , but in practice experiments by Huppert *et al.* have shown that  $\text{Fr}_f = 1.19$  for particulate gravity currents.[1]

Assume that  $h_N = h$  and  $u_N = u$ . We must solve these equations for  $\phi$  and  $L$ , subject to some initial conditions  $L = L_0$  and  $\phi = \phi_0$  at  $t = 0$ . One way to proceed would be to eliminate one of  $\phi$  or  $L$ , and get the equation

$$\frac{d}{dt} \left[ L \left( \frac{dL}{dt} \right)^2 \right] = -\frac{u_s L}{h} \left( \frac{dL}{dt} \right)^2 \quad (6.4.5)$$

which must be solved numerically. We can also make progress by dividing one equation by the other, to get

$$\frac{d\phi}{dL} = -\frac{u_s L}{h} \frac{1}{\text{Fr}_f (\phi g_0' h)^{1/2}} = -\frac{\phi^{1/2} L^{3/2}}{\beta} \quad (6.4.6)$$

where

$$\beta = \frac{\text{Fr}_f (g_0' M^3)^{1/2}}{u_s} \quad (6.4.7)$$

Equation 6.4.6 can be solved easily:

$$L^{5/2} = L_0^{5/2} + 5\beta \left( \phi_0^{1/2} - \phi^{1/2} \right) \quad (6.4.8)$$

The current stops advancing when the concentration drops to  $\phi = 0$ . Hence the run-out length of the current  $L_\infty$  is

$$L_\infty^{5/2} = L_0^{5/2} + 5\beta \phi_0^{1/2}. \quad (6.4.9)$$

We can therefore rearrange (6.4.8):

$$\frac{\phi}{\phi_0} = \left[ 1 - \left( \frac{L}{L_\infty} \right)^{5/2} \right]^2 = \left[ 1 - \xi^{5/2} \right]^2 \quad (6.4.10)$$

where  $\xi = L/L_\infty$ . Having found  $\phi$  in terms of  $L$  and  $L_\infty$ , we can solve (6.4.4) implicitly for  $t$  as a function of  $L$ .

## 6.5 Sediment transport

Particles in a fluid can move by several means. Particles which are in suspension (the *suspended load*) or which have dissolved (the *dissolved load*) will move with the flow. Particles which have settled to the bottom of the fluid can roll or slide along the bottom, or by hopping (*saltation*). In a river, silt and clay tend to move by suspension; sand particles, which are larger, by saltation; gravel, larger still, by rolling and sliding.

A particle out of suspension does not necessarily move when there is a flow. A rock on the bed starts to move only when the flow exerts a critical shear stress on the bed. However, if the flow is turbulent then a sudden eddy may be able to move the rock: turbulent flows are stochastic, and need to be modelled as such.

Transport will change the morphology of the bed by erosion deposition: a strong flow can break up large rocks into smaller pieces. This in turn changes whether these particles are able to be suspended or settle out of suspension.

### 6.5.1 Resuspension

Resuspension is the process by which particles which have settled to the bottom boundary are lifted back up into suspension in the fluid. A flow near a boundary obeys the no-slip condition at the boundary, but away from the boundary suppose the velocity is uniform, horizontal, with speed  $U$ . There is a viscous sublayer of thickness  $\delta \sim \nu/U$  near the boundary, where the speed drops from  $U$  to 0. The velocity profile in the viscous sublayer is approximately linear. The shear stress on the boundary is  $O(\mu U/\delta) = O(\rho U^2)$ .

Consider a particle deposited in the viscous sublayer. Since the fluid at the top of the particle moves faster than the fluid at the bottom, then by Bernoulli's principle the pressure at the bottom of the particle is higher than the pressure at the top. This causes *lift*. If the particle is more dense than the fluid, then it also experiences a 'downwards' *buoyancy* force.

## 6.6 Aqueous and aeolian bedforms (dunes)

## 6.7 Dry granular flows, rheology, segregation

Granular materials do not fill the space that they occupy, but instead have a *packing fraction*  $\phi$ . The packing fraction is variable for a given material: a collection of uniform rigid spheres has a maximum packing fraction of  $\phi \approx 0.74$ , but randomly packed spheres have typically  $\phi \approx 0.64$ . The value of the packing fraction depends on the history of the material: that is, how it came to be arranged as it is. A pile of sand could have very different packing fractions depending on whether the sand was simply poured onto a surface, or slowly added and packed together.

Like a viscous fluid, a granular flow on a inclined plane or chute executes a shear flow  $u = U(z)$ . But unlike a viscous fluid, the cross-depth velocity profile  $U$  is not quadratic in  $z$ , and the shear stress  $\tau_{xz}$  is not linearly proportional to the shear rate  $\dot{\gamma} = U'(z)$ . Bagnold (1954) showed by simple collisional arguments and through experiments that, for spherical grains,  $\tau_{xz}$  is in fact proportional to  $\dot{\gamma}^2$ .<sup>8</sup> This stress-strain relation would give rise to what is called the *Bagnold velocity profile*.

Bagnold (1954) also showed that the grains also exert a normal stress  $\tau_{zz}$  on each other, owing to their collisions; this serves to

---

<sup>8</sup>Bagnold's experiments were conducted with a suspension of grains in a viscous fluid. At high shear rates, the viscosity of the fluid could be neglected, compared to the inertia of the grains, and  $\tau_{xz} \propto \dot{\gamma}^2$ . At low shear rates, this simply behaves as a particle-laden viscous flow;  $\tau_{xz} \propto \dot{\gamma}$  but with a higher effective viscosity as discussed above.

The Bagnold relation  $\tau_{xz} \propto \dot{\gamma}^2$  was derived for this particular geometry. There have been subsequent attempts to find more general constitutive relations for dense granular flows. This study is called *rheology*. A recently-developed theory is that of Jop *et al.* (2006), the  $\mu(I)$  rheology. In the  $\mu(I)$  rheology, the shear stress  $T$  is taken to be equal to  $\mu(I)P$ , where  $P$  is the pressure (normal stress). The coefficient of friction  $\mu$  is taken to be a function of the *inertial number*  $I = \dot{\gamma}d(P/\rho_s)^{1/2}$ , a nondimensionalised shear rate.[3]

A granular flow with particles of different sizes or densities will exhibit *segregation*. Larger particles will tend to come to the top or edges of the flow. We can demonstrate this by shaking a jar containing sand and marbles.



# Bibliography

- [1] Herbert E. Huppert. Quantitative modelling of granular suspension flows. *Phil. Trans. R. Soc. Lond. A*, 356:2471–2496, 1998.
- [2] Ralph Alger Bagnold. Experiments on a gravity-free dispersion of large solid spheres in a newtonian fluid under shear. *Proceedings of the Royal Society of London. Series A, Mathematical and Physical Sciences.*, 225(1160):49–63, August 1954.
- [3] Pierre Jop, Yoël Forterre, and Oliver Pouliquen. A constitutive law for dense granular flows. *Nature*, 441, 2006.